



CHALMERS
UNIVERSITY OF TECHNOLOGY

Assembly and disassembly of the influenza C matrix protein layer on a lipid membrane

Master's thesis in Biomedical Engineering

BIRGER EKLUND

Department of Applied Physics
CHALMERS UNIVERSITY OF TECHNOLOGY
Gothenburg, Sweden 2016

MASTER'S THESIS 2016

**Assembly and disassembly of the influenza C
matrix protein layer on a lipid membrane**

BIRGER EKLUND



Department of Applied Physics
Division of Biological Physics
CHALMERS UNIVERSITY OF TECHNOLOGY
Gothenburg, Sweden 2016

Assembly and disassembly of the influenza C matrix protein layer on a lipid membrane
BIRGER EKLUND

© BIRGER EKLUND, 2016.

Supervisor: Marta Bally, Applied Physics
Examiner: Marta Bally, Applied Physics

Master's Thesis 2016
Department of Applied Physics
Division of Biological Physics
Chalmers University of Technology
SE-412 96 Gothenburg
Telephone +46 31 772 1000

Typeset in L^AT_EX
Printed by Chalmers Reproservice
Gothenburg, Sweden 2016

Assembly and disassembly of the influenza C matrix protein layer on a lipid membrane

BIRGER EKLUND

Department of Applied Physics

Chalmers University of Technology

Abstract

Insight into the inner workings of viruses is an important piece of knowledge in humanity's expanding collection of knowledge which can potentially be used to treat or prevent diseases. Influenza C is known to cause an infection with cold-like symptoms with possible complications in young children. The virus is a lipid-enveloped RNA virus in the Orthomyxoviridae family and incorporates 9 proteins. One of these is matrix protein 1 ($M1_C$) which is found on the inside of the lipid-envelope of the virion. Influenza C in general and $M1_C$ in particular have not been extensively studied. However, influenza A and its matrix protein 1 have been studied to a great extent.

In this thesis the binding and release of $M1_C$ on supported lipid bilayers (SLB) in various environments have been investigated. The SLB is a basic model of the lipid envelope of the influenza virions which is also suitable for the two surface-based techniques used in this work. The two main environmental factors that were varied were the salinity and pH of the surrounding solution. The protein-protein and protein-bilayer binding behaviours were the two main interactions examined.

In the Quartz Crystal Microbalance with Dissipation monitoring (QCM-D) the amount of $M1_C$ bound to an SLB was measured. Information on the adlayer's viscoelastic properties was also obtained. With this technique it was revealed that the binding of the protein is highly dependent on electrostatic charges.

In the microscope, fluorescence and Surface Enhanced Ellipsometric Contrast (SEEC) microscopy was used to observe the spatial arrangement of the $M1_C$ on the SLB. The SEEC microscopy was used to observe aggregations of $M1_C$ on the SLB. A fraction of the negatively charged lipids in the SLB were tagged with the fluorescent dye NBD and the clustering of these was observed with fluorescence microscopy. This combined with the SEEC observations gave the conclusion that the proteins aggregate on the SLB and recruit negatively charged lipids.

This work found that the main binding strategy for $M1_C$ is to utilise electrostatic forces. This is important because this binding is used both in the forming of the virions and for maintaining the structural integrity of the virion. It was also found that endosomal pH leads to some dissociation of $M1_C$ from the lipid bilayer. This is important since the dissolution of the virion's matrix protein layer in the endosome has been shown to be vital for infection in influenza A.

Keywords: influenza, virus, M1, matrix protein, SLB, QCM-D, SEEC, TIRF.

Acknowledgements

I would like to begin with stating that this thesis has been an important learning experience for me. I have gained insight into self management, experimental techniques, and scientific methodology. Here follows, in no particular order, the people who have contributed to the completion of this thesis directly or indirectly.

I would like to thank the Biological Physics group for always being willing to help, amusing coffee breaks, and a joyful work camaraderie.

I would like to thank my supervisor Marta Bally for her tenacious support, constructive criticism, and remarkable ability to always be available for conversation and consultation.

I would like to thank my friends at school for supporting me and sharing my struggle, and my friends outside school for providing much needed distraction.

Finally, I would like to thank my parents for encouraging and supporting me through my many years of education.

Birger Eklund, Gothenburg, May 2016

Contents

List of Figures	viii
1 Introduction	1
1.1 Context	1
1.2 Gap	1
1.3 Aim	2
1.3.1 Research Questions	2
2 Theory	3
2.1 Influenza virus	3
2.1.1 Life cycle of the influenza virus	5
2.2 Matrix protein 1 (M1)	5
2.3 Supported Lipid Bilayer formation	6
3 Materials and Methods	9
3.1 Materials	9
3.2 Quartz Crystal Microbalance with Dissipation monitoring	10
3.2.1 Theoretical background	11
3.2.2 Forming a supported lipid bilayer in the QCM-D	11
3.2.3 Protein adsorption and removal in the QCM-D	12
3.3 Microscopy	14
3.3.1 Fluorescence microscopy	14
3.3.2 Surface Enhanced Ellipsometric Contrast	15
3.3.3 Forming a supported lipid bilayer for the microscopy experiments	15
3.3.4 Protein adsorption and dissolution on the microscope	17
4 Results	19
4.1 Quartz Crystal Microbalance with Dissipation monitoring	19
4.1.1 Initial binding is charge dependent	22
4.1.2 Attempted protein layer dissolution	22
4.2 Fluorescence microscopy & Surface Enhanced Ellipsometric Contrast (SEEC) microscopy	25
4.2.1 Externally induced changes on protein aggregate morphology	27
4.2.2 Diffusive behaviour of DOPS	27

5	Discussion	33
5.1	Protein binding	33
5.1.1	Protein-lipid binding	33
5.1.2	Aggregation	34
5.1.3	QCM-D dissipation changes during binding	34
5.2	Dissociation	34
5.2.1	Charge-dependent dissociation	35
5.2.2	pH-dependent dissociation	35
5.3	Future research	36
	Bibliography	36
A	Supporting information	I

List of Figures

2.1	Schematic image of the structure of an influenza C virion	4
2.2	Schematic of the influenza virus life cycle	4
3.1	The two instruments used in this thesis	9
3.2	The appearance and basic operation of the QCM-D crystal	10
3.3	Frequency and dissipation change as measured with QCM-D of lipid vesicles adsorbing onto a crystal and bursting to form an SLB	12
3.4	Resonance frequency shift (ΔF) as measured by QCM-D displaying the phases of a binding and dissolution experiment	14
3.5	A schematic sketch of the principle behind SEEC	16
3.6	TIRF microscopy images of an SLB, and a layer of lipid vesicles	16
4.1	QCM-D data of SLB formation, binding and release of protein	20
4.2	Change of frequency as measured with QCM-D of full-length and N-terminal M1 _C binding and releasing	20
4.3	Change of dissipation as measured with QCM-D while binding and rinsing full-length and N-terminal M1 _C	21
4.4	D-F plots of the two data sets from figures 4.2 and 4.3	21
4.5	Change of frequency as measured with QCM-D for the binding and release of full-length M1 _C in different environments	23
4.6	Box plots of the percentage of the irreversibly bound protein that was removed by changing the properties of the surrounding buffer	24
4.7	TIRF and SEEC microscopy images taken before and after adsorption of N-terminal protein	25
4.8	TIRF microscopy images of full-length protein aggregates	26
4.9	TIRF microscopy image of N-terminal protein aggregates	26
4.10	TIRF images of full-length protein aggregations observed while reacting to a buffer change	28
4.11	TIRF images of N-terminal protein aggregations observed while reacting to a buffer change	29
4.12	TIRF images of full-length M1 _C being exposed to pH 4.9	29
4.13	Fluorescence images of a photobleached lipid bilayer containing fluorescently labelled DOPS and with adlayered full-length protein clusters	30
4.14	TIRF and SEEC images of a photobleached bilayer containing DOPS-NBD and with adlayered protein clusters	31
A.1	QCM-D data of N-terminal M1 _C during binding and release.	I

1

Introduction

1.1 Context

The seasonal influenza is a viral infection that causes fever, sore throat, headache, cough, and other symptoms. It can also lead to complications in the form of a number of respiratory-tract illnesses such as pneumonia. It is estimated that 3-5 million severe cases of influenza occur annually. These lead to at least 250'000 deaths globally each year. There are three types (genera) of influenza, denoted types A, B, and C. The more severe consequences of the seasonal influenza are caused by type A and B influenza viruses [1, 2]. Influenza C virus instead causes symptoms very similar in kind and severity to those of the common cold [2, 3]. It is more dangerous to small children and most humans acquire antibodies against it at an early age [4].

The influenza virus is a lipid-enveloped RNA virus encoding 11-14 (types A and B) or 9 (type C) proteins. A matrix protein M1 is found in all three virus types, but the amino acid sequence varies significantly [5]. In influenza A, the M1 protein ($M1_A$) has been suggested as the connector between the lipid bilayer and the ribonuclear proteins (RNP) constituting the genetic core of the virus. It has also been shown to bind hemagglutinin and neuraminidase [6, 7], two important surface proteins in influenza A and B which are replaced by hemagglutinin-esterase fusion in influenza C. These roles as a connecting and binding protein combined with it inducing budding of lipid bilayers has inferred $M1_A$ as vital both for forming the new virions and supporting them structurally [8]. For a more comprehensive description of the influenza virus see section 2.1.

1.2 Gap

Influenza C is the least devastating kind of influenza. It is very seldom reported as a cause for human illness at all. It does infect humans, mostly children, but the illness caused is often subclinical [2, 4]. These circumstances probably contribute to the fact that influenza C is the least researched kind of influenza.

For this thesis this is a double-edged sword. On one hand it makes it harder to find references and articles to compare with, therefore most often comparisons will be made with influenza A. On the other hand it makes this thesis more relevant simply because of the scarcity of the work done on influenza C.

1.3 Aim

The aim of this work has been to characterise the behaviour of M1 from influenza C ($M1_C$) while interacting with lipid membranes in the form of supported lipid bilayers (SLB). This includes characterising the binding and release of the protein, and also its dissolution in well-defined environments. Further aspects that have been studied are the assembly and clustering of $M1_C$ on the SLB.

1.3.1 Research Questions

- How does the binding of the N-terminal part of $M1_C$ compare to the one of the full-length protein? It has been found that the N-terminal of influenza A is the part of the protein that binds to lipids. The same study also found that the C-terminal on the other hand binds to RNPs [6], a mechanism that is not addressed by this work.
- Can $M1_C$ bind to uncharged lipids? A recent article claims that M1 from influenza A does not require any negatively charged lipids in a bilayer to bind to it [9]. Should it become apparent that $M1_C$ is not able to bind to uncharged lipids this would be an interesting distinction between it and its counterpart in influenza A.
- Can $M1_C$ bind to lipids in a solution with a high salt concentration? If that is not the case this suggests that the initial binding is strictly electrostatic. It has been shown that M1 in influenza A has a large electrostatic component to its binding [10].
- If the binding of $M1_C$ is hindered by a high salt concentration, will it be removed by the same if bound at a low concentration? If not, this suggests that there is some mechanism of binding other than electrostatic forces that is not affected by ion concentration.
- How does $M1_C$ react to low pH? Cryo-electron microscopy and cryo-electron tomography have been used to show that M1 from influenza A dissociates from the lipid bilayer of the virion after 5 min in moderately low pH (4.9) [11]. This is the pH that the virion will encounter in the endosome during entry.
- Does the full-length and N-terminal $M1_C$ have the same clustering properties when binding to a lipid bilayer? The C- and N-terminal protein of influenza A have distinctive oligomerisation tendencies in solution, both for neutral and weakly acidic pH [12]. Whether these tendencies exist in influenza C, and whether they are expressed also for proteins bound to lipid bilayers, is not confirmed.

2

Theory

There are three major subjects that the reader should be acquainted with in order to fully appreciate the results in this thesis. Some understanding of the structure and behaviour of the influenza virus is needed to understand the role of M1 therein. Some understanding of the matrix protein M1 is needed since this is the main subject of study. Since all experiments have been done on SLBs, a rudimentary understanding of these is also needed. The purpose of this chapter is to supply the necessary background information on these three topics.

2.1 Influenza virus

Influenza is an RNA virus of the orthomyxovirus family. Like all viruses it infects healthy cells, reproduces in them, and then spreads to other cells. For the virus to spread from infected cells to healthy ones, the infected cell needs to produce a virion. The virion is an extracellular vesicle, in influenza either oblong and filamentous or roughly spherical, equipped with all proteins and genetic material needed to infect a healthy cell. The production of the virion is known as viral budding.

The influenza virion is essentially a lipid bilayer envelope containing an assortment of proteins. In the lipid bilayer, the two proteins hemagglutinin (HA) and neuraminidase (NA) are found with the majority of each protein protruding to the outside of the virion. These proteins are the parts of the virion that interact with cells; NA facilitates release of the virion from the surface of the parent cell by enzymatically cleaving sialic acid receptors and HA is the main actor when it comes to infecting new cells as it mediates binding to sialic acid. In influenza C, these two proteins are replaced by a combination protein called hemagglutinin-esterase fusion (HEF) [13], see figure 2.1 for the complete structure of influenza C. Also found in the envelope is the ion channel CM2. The M1 protein is found at the inner leaflet of the envelope, see section (2.2) for a more comprehensive description. Inside the virion the viral RNA is found, this is the most crucial constituent for the reproduction of the virus. The RNA is closely associated with nucleoproteins (NP), forming RNP. The RNPs are needed to infect a cell nucleus to hijack it and start producing more virions. These are not all of the proteins present in the influenza virion, but all that the rest of this report will require the reader to be aware of.

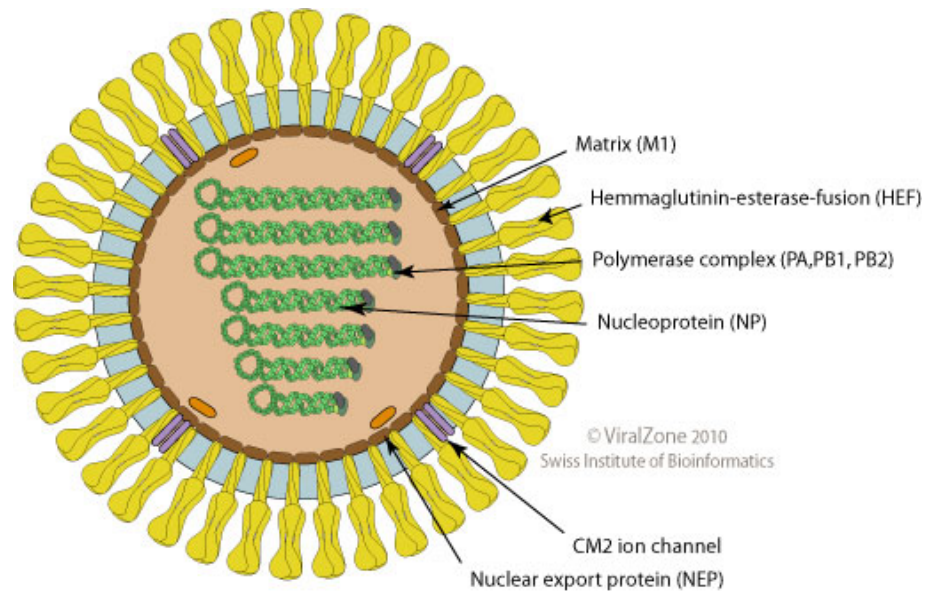


Figure 2.1: Schematic image of the structure of an influenza C virion. The lipid bilayer is represented in bright blue, with the M1_C protein (in dark brown) attached on the inside. Image from *viralzone.expasy.org*

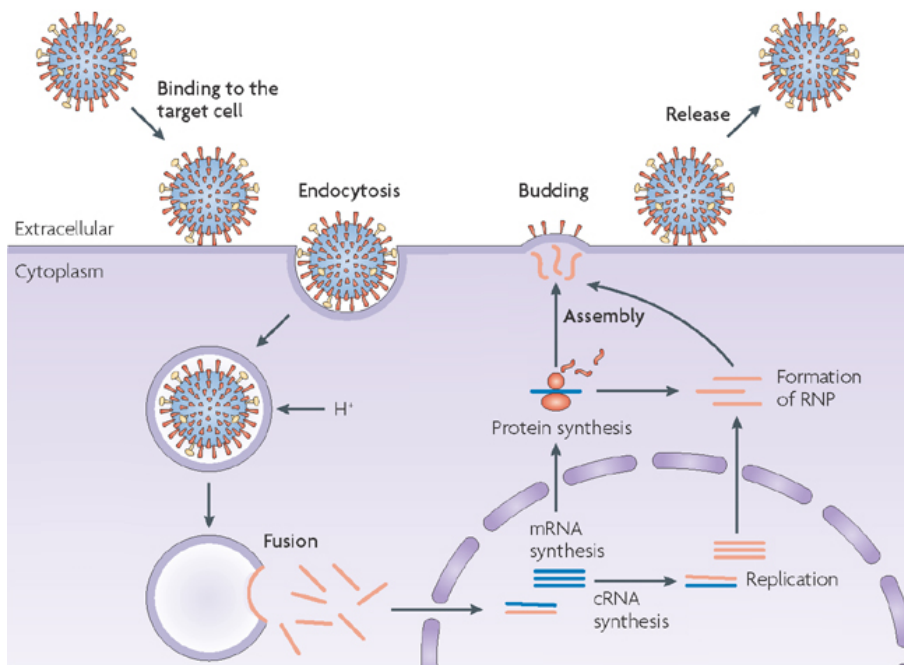


Figure 2.2: Schematic of the influenza virus life cycle. Image adapted from Itzstein [14].

2.1.1 Life cycle of the influenza virus

The influenza virus life cycle starts with a virion attaching to a healthy cell; this process is mediated by HA in influenza A and B and by HEF in influenza C, see figure 2.2 for the complete life cycle of influenza. The virion is then engulfed via endocytosis by the target cell. Upon acidification of the endocytic compartment, the pH in the interior of the virion is lowered by the ion channels M2 or CM2 in influenza A and C respectively [15, 16]. It has been found that this change in pH is crucial for the infection process of influenza A. For example, hemagglutinin undergoes large conformational changes and M1_A dissociates from both the lipid envelope [17] and the RNPs [18]. Eventually the virion and the endosome fuses and the contents of the virion is released into the cytoplasm. The viral RNA is transported into the nucleus and induces the production of more viral proteins, the details of this process is of no great importance to this thesis. The new viral proteins are transported to the surface of the host cell where they assemble into a new virion which buds out from the cell wall. Both the assembling of the viral proteins and the budding of the virion has been inferred to be dependent on M1 in influenza A [8]. Finally, the virion separates itself from the host cell and is ready to infect a new healthy cell. For more information on the life cycle of influenza A, see the review by Rossman and Lamb [19].

2.2 Matrix protein 1 (M1)

The central subject of this thesis is the M1_C; a truncated version containing the N-terminal part only has also been examined. The full-length M1_C is a 27 kDa protein comprised of 242 amino acids [5], the N-terminal of the protein used in this project has a ~17.4 kDa mass and is 155 amino acids long [20]. It has been reported that the N-terminal and the C-terminal parts of the M1 protein of influenza A have different oligomerisation characteristics at neutral and low pH [12]. This might lead to differences in binding characteristics between the full-length protein and the N-terminal, particularly in the spatial binding behaviour.

M1 from influenza A has been found to interact with HA and NA, both at the cell membrane and while in transit from the cell cytosol to the budding site [7]. These results have been corroborated by findings that both virion forming and the assembly of the virion components is delayed in cells infected with viruses that were mutated to produce fewer M1 [21].

Also in influenza A, M1 has been shown to form a monolayer on the inside of the virion membrane. This has been shown by cryo-electron microscopy and cryo-electron tomography in which a very thin layer of protein was observed at the inner leaflet of the lipid bilayer of virions [11]. Through electron micrograph observations and investigations of the impact of a high-salt environment, this binding has been attributed mainly to electrostatic forces [6, 10], although contributions from other types of interactions can not be fully dismissed [22]. The proportion of M1 in oligomers compared to monomers have also been found to be higher in close proximity to lipid membranes [9]. However, to date it is not clear whether this observation is attributed to a stronger oligomer-membrane interaction or to bilayer-

induced oligomerisation.

By trying to generate virus-like particles while suppressing the expression of different viral components, it has been shown that M1 is the only one that is essential for virion formation in influenza A [23]. It has also been found to be instrumental in controlling whether the progeny virions are filamentous or spherical [24]. In influenza C the role of M1_C has not been as thoroughly examined but the protein has been found capable of producing membrane tubules without any other viral components [25]. It has also been found that it could be responsible for the shape of the virions, with a single amino acid mutation determining its morphology (spherical or filamentous) [26].

It has been shown several times that changes in pH between 4.0 and 7.5 are vital for M1 from influenza A to be able to perform its multiple functions [11, 17, 18, 27–29]. The fact that changes in pH are very important for the spreading of the virus as a whole makes it interesting to study how M1_C reacts to varying pH. M1 from influenza A has been examined in solution for pH 7.4 and 5.0. The full-length M1_A showed various oligomers at pH 7.4, with dimers being the smallest ones. The oligomers dissociated into dimers when the pH was lowered to 5.0. The two halves of the protein were examined separately and the N-terminal was found in multiple-order oligomers at pH 7.4 but dissociated into monomers at pH 5.0. The C-terminal on the other hand was found as a stable dimer at both pH 7.4 and 5.0 [12]. When examined with surface plasmon resonance, on a lipid membrane surface mimicking the virion envelope, the findings included a partial protein desorption when acidifying the environment to pH 4 for a protein layer adsorbed at pH 7 [27]. A study of complete virions with cryo-electron tomography found that M1 was generally present as a layer on the inside of lipid membrane at pH 7.4. When incubated in pH 4.9 for 30 min most virions had lost this layer [28].

2.3 Supported Lipid Bilayer formation

A large portion of the current knowledge of biological phenomena at cell membranes comes from research done on membrane models or mimics. These models are based on the self-assembly of one of the membrane's major components, the phospholipids. These are amphiphilic, meaning that they have both a hydrophobic side and a hydrophilic side. If put in water, they will spontaneously self-assemble into bilayers with the hydrophilic heads facing the water and the hydrophobic tails tucked together inside. A unique characteristic of lipid bilayers is that the individual lipids are mobile within it, while the general structure of the bilayer is unaltered [30]. When in contact with an aqueous solution, these bilayers tend to form liposomes, which are bilayer spheres, with one hydrophilic side of the bilayer facing the solution in the liposome interior and the other hydrophilic side of the bilayer facing the bulk solution on the outside of the liposome. When in contact with specific surfaces, such as glass, vesicles will spontaneously rupture to form a so-called SLB.

An SLB is a lipid bilayer deposited on a solid support which, compared to other lipid bilayers, it is easily constructed and very stable. It can be formed from a group of liposomes tightly clustered on a plane solid surface and its composition is very versatile [30, 31]. This is the method chosen in this thesis to create a mimic of the

cell membrane. Since it is flat and robust, an SLB is particularly suitable for surface sensitive techniques and microscopy. Like the cell membrane it is mimicking, an SLB can contain an assortment of proteins and be composed of a variety of lipids.

Since the purpose of this thesis is to examine the interaction of $M1_C$ with a lipid bilayer, the choice was made to exclude all other influenza proteins from the experiments. This makes the signal from the $M1_C$ easier to observe, it ensures that the reactions observed are actually between $M1_C$ and bilayer or between $M1_C$ proteins since there is nothing else to react with, and it makes the setup of the experiments easier. The diversity of the lipid composition was also decreased from what would be expected in the natural case, this was done mostly to simplify the process of adjusting the characteristics of the bilayer. The form of the bilayer was chosen as SLB because it is compatible with the chosen experimental techniques. The contents of the SLBs used in this thesis are described in section 3.1 and their construction is described in sections 3.2.2 and 3.3.3.

3

Materials and Methods

Two main research devices are used in this thesis. The first is the Q-Sense E4 Quartz Crystal Microbalance with Dissipation monitoring (QCM-D), which is used to measure the mass and indicate structural changes of adsorbed protein, this is described in section 3.2. The second instrument used is the Nikon ECLIPSE Ti Inverted Research Microscope which is used to image the protein binding to and aggregating on the lipid bilayer, this is described in section 3.3. Both of these are shown in figure 3.1. The materials used in the thesis are described in section 3.1.

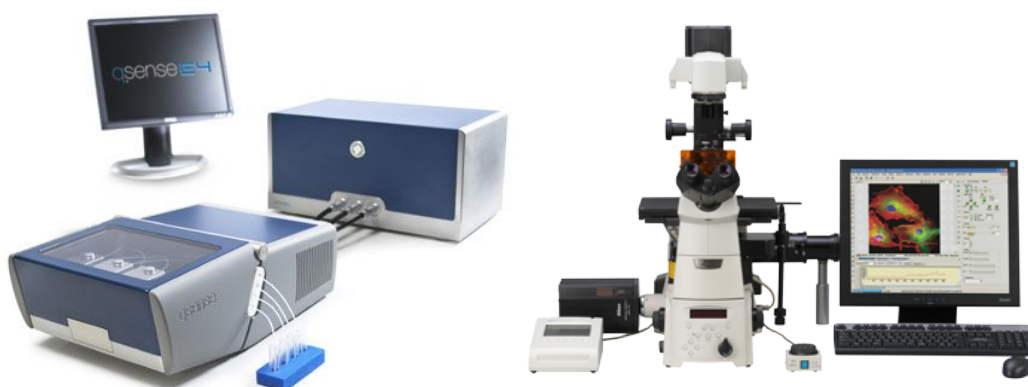


Figure 3.1: *The two instruments used in this thesis, to the left, a Q-Sense E4 Quartz Crystal Microbalance with Dissipation monitoring (QCM-D, image from biolinscientific.com) and to the right, a Nikon ECLIPSE Ti Inverted Research Microscope (image from nikon.com).*

3.1 Materials

During the course of this thesis several buffers have been used for various purposes, their compositions are presented in table 3.1. Buffers 2 and 3 were made by adding 5 mM CaCl and 10 mM EDTA respectively to buffer 1, therefore their pHs are not specified.

The N-terminal protein used in this thesis was extracted from the strain C/Ann Arbor/1/1950; this and the full-length protein was obtained through collaboration with Winfried Weissenhorn (EMBL, Grenoble).

The SLBs both in the QCM-D and on the microscope were formed using lipid vesicles. These vesicles were made by adding lipids diluted in chloroform into a round bottom flask, the chloroform was then evaporated first by a nitrogen flow and then

#	Buffer	Salt	pH	Extra
1	10 mM Hepes	150 mM NaCl	7.5	
2	10 mM Hepes	150 mM NaCl 5 mM CaCl		
3	10 mM Hepes	150 mM NaCl		10 mM EDTA
4	10 mM Hepes	50 mM NaCl	7.5	
5	10 mM Hepes 10 mM citric acid	50 mM NaCl	4.9	
9	10 mM Hepes	950 mM NaCl	7.5	

Table 3.1: *Compositions of the buffers used in this thesis.*

by a vacuum pump for at least three hours. The dried lipids were then resuspended in buffer 1 (see table 3.1) and extruded 11 times through 30 nm pores. The SLBs in this thesis have exclusively been made from the two phospholipids 1,2-dioleoyl-sn-glycero-3-phosphocholine (DOPC) and 1,2-dioleoyl-sn-glycero-3-phospho-L-serine (DOPS). Only the unlabelled version of DOPC was used while both a version labelled with nitrobenzoxadiazole (1-oleoyl-2-12-[(7-nitro-2-1,3-benzoxadiazol-4-yl)amino]dodecanoyl-sn-glycero-3-phosphoserine), DOPS-NBD) and an unlabelled version of DOPS was used. Two different lipid composition were used in the QCM-D: 70 % DOPC, 30 % DOPS; and 100 % DOPC. For microscopy experiments, the lipid composition was: 70/101 DOPC, 30/101 DOPS, and 1/101 DOPS-NBD.

Both the crystals used in the QCM-D and the slides used for microscopy were SiO₂ coated. The crystals were purchased from Q-Sense and the slides were purchased from Nanolane.

3.2 Quartz Crystal Microbalance with Dissipation monitoring

A QCM-D is a device that can measure the mass and rigidity of adsorbate on the surface of a quartz crystal. The mass is found by monitoring the change in the resonance frequency of an excited piezoelectric crystal and its overtones, see figure 3.2 for an illustration. The oscillation over the crystal is turned off and the dissipation of this oscillation is measured. This in combination with the mass can be used to find the the rigidity of the adsorbate.



Figure 3.2: *Illustration of the appearance and basic operation of the QCM-D crystal. Image from [32]*

At the heart of the QCM-D is a quartz crystal connected to an electrical circuit

and placed in a flow cell. The circuit is used to find the crystals resonance frequency and/or some of its overtones, and monitor these.

3.2.1 Theoretical background

If all other parameters are kept constant, a change in one of the resonance frequencies corresponds to a change of the oscillating mass which in most cases will be the result of adsorbed mass on the surface of the crystal [33]. If the film adsorbed on the surface is rigid and thin, the change of mass (Δm) has been shown to be proportional to the change of frequency (ΔF):

$$\Delta m = -C \frac{\Delta F}{n} \quad (3.1)$$

where $n = (1, 3, 5, \dots)$ is the observed overtone [34] and C is a crystal-dependent, positive, mass sensitivity constant. This is the Sauerbrey equation.

In the QCM-D, in addition to resonance frequency, the dissipation of the quartz crystal is also monitored. The dissipation D is defined as:

$$D = \frac{E_{\text{dissipated}}}{2nE_{\text{stored}}} \quad (3.2)$$

where E_{stored} is the total energy stored in the oscillation and $E_{\text{dissipated}}$ is the energy dissipated during one period of the oscillation [35]. One way to measure D is to turn off the driving voltage to the crystal and observe the voltage induced by the the crystal oscillation as it decays. This can then be fitted to the following function, and the dissipation can be found from the relation:

$$A(t) = A_0 e^{-\frac{t}{\tau}} \sin(2\pi ft + \alpha) \quad D = \frac{1}{\pi f \tau} \quad (3.3)$$

The dissipation is not a direct measurement of rigidity and will in this thesis only be used to compare protein binding qualitatively. In section 3.2.2 it will be described how the dissipation was used during the QCM-D experiments to verify whether bilayer formation was complete.

All QCM-D experiments in this thesis were done on the same type of crystal (same C) and all data presented in this thesis report is from the second overtone ($n = 5$). This means that an increase of mass coupled to the crystal is proportional to a decrease in the resonance frequency, as can be seen in equation 3.1. For the rest of the report, whenever a change of mass is discussed in relation to the QCM-D, it will describe a proportional change of frequency.

3.2.2 Forming a supported lipid bilayer in the QCM-D

To form an SLB in the QCM-D the lipid vesicles described in section 3.1 were used. The concentration of vesicles used to make the SLB was 0.1 mg/ml. The crystals were cleaned with SDS, rinsed with water and UV/ozone cleaned immediately before use. The flow cells were cleaned with Hellmanex III detergent (2% by volume in water) and rinsed with water.

Since SiO_2 surfaces are known to acquire a negative surface charge density and the most commonly used lipid composition in this thesis has a net negative charge, Ca^{2+} were used as linking ions. Therefore the vesicles were diluted in buffer 2, prior to being injected into the QCM-D flow cell. The SLB was formed in a buffer with 150mM NaCl, 5mM CaCl, and pH 7.5 (buffer 2). After the SLB was formed the Ca^{2+} ions were rinsed off with EDTA (buffer 3).

During the adsorption of the vesicles on the crystal, both resonance frequency and dissipation are monitored. If at the end of this process the total change in dissipation is small enough ($\Delta D < 0.7 \cdot 10^6$), the vast majority of the vesicles are considered to have burst and the bilayer was considered of sufficient quality to carry out the measurement [30, 36]. An example of the bilayer formation process can be seen in figure 3.3.

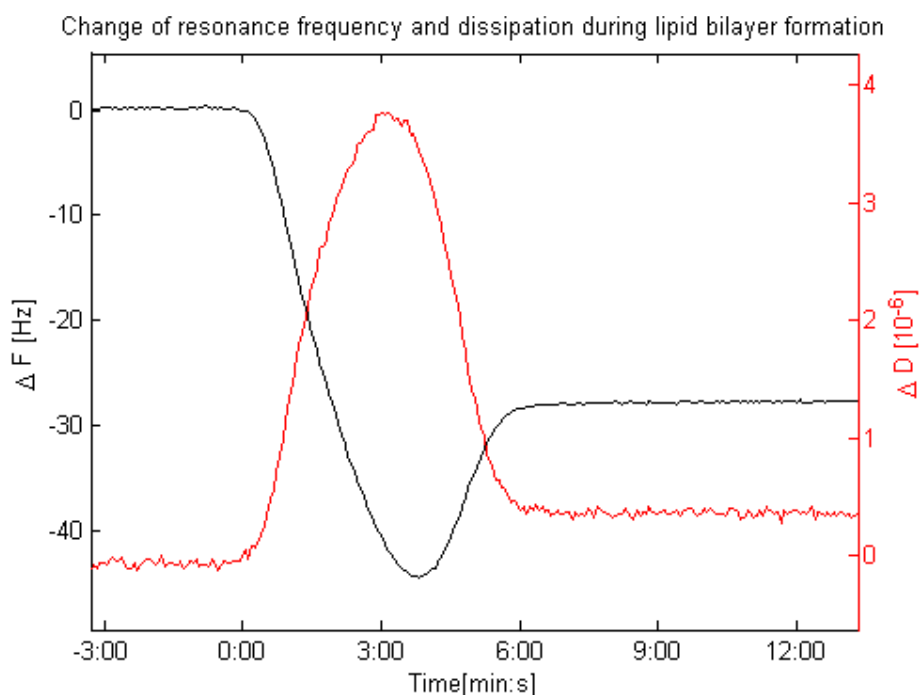


Figure 3.3: Frequency and dissipation change as measured with QCM-D of lipid vesicles adsorbing onto a crystal and bursting to form a Supported Lipid Bilayer (SLB). At time 0:00 the lipid vesicles start adsorbing intact to the surface leading to a mass increase on the crystal. Because the vesicles are soft and filled with buffer the dissipation also increases dramatically. At time ~4:00 the vesicles have reached a critical coverage and start bursting into the SLB. The mass coupled to the crystal decreases, mostly from buffer being released. The dissipation also decreases greatly since the adsorbed SLB is more rigid than the buffer-filled vesicles.

3.2.3 Protein adsorption and removal in the QCM-D

The QCM-D was used to measure the binding of M1_C to the SLB in different environments. Unless otherwise noted, in all experiments the protein was allowed to

bind to an SLB composed of 70% DOPC (net neutrally charged) and 30% DOPS (negatively charged). The binding of the protein occurred in a buffer with 50 mM NaCl (buffer 4). Two other environments were occasionally investigated: binding to a 70% DOPC, 30% DOPS lipid bilayer in 150 mM NaCl (buffer 1); and binding to a 100% DOPC lipid bilayer in 50 mM NaCl (buffer 4). The purpose of these experiments was to test the proteins dependence on electrostatics for binding. All of these binding experiments were performed under physiological pH, i.e. at pH 7.5.

The amount of full-length and N-terminal protein added was 5 μg and 7 μg respectively in concentrations of 10 $\mu\text{g}/\text{ml}$ (~ 345 nM) and 12 $\mu\text{g}/\text{ml}$ (~ 690 nM). The amount of protein bound after rinsing was represented by the measurement designated "Irreversibly bound protein", which is the difference in resonance frequency between before the protein was added and after the rinsing of the protein has stabilised, see figure 3.4. In zone B a certain amount of protein is bound, part of this is rinsed in zone C. The irreversibly bound protein is what is left when this rinsing has stabilised. Since the QCM-D monitors both resonance frequency and dissipation not only the amount of protein adsorbed to the SLB was detected but also its rigidity or structural changes [37].

The possible release of the protein at high ionic strengths or low pH, was also tested. The higher NaCl concentrations were chosen as 150 mM (buffer 1) and 950 mM (buffer 9). The low pH 4.9 (buffer 5) was chosen to emulate the conditions in the endosome, that has been shown to affect M1_A [17, 28]. To do these experiments, the chosen buffer was flown through the QCM-D cell at 50 $\mu\text{l}/\text{min}$ for 30 min. These experiments have been performed with both full-length and N-terminal M1_C to compare their properties.

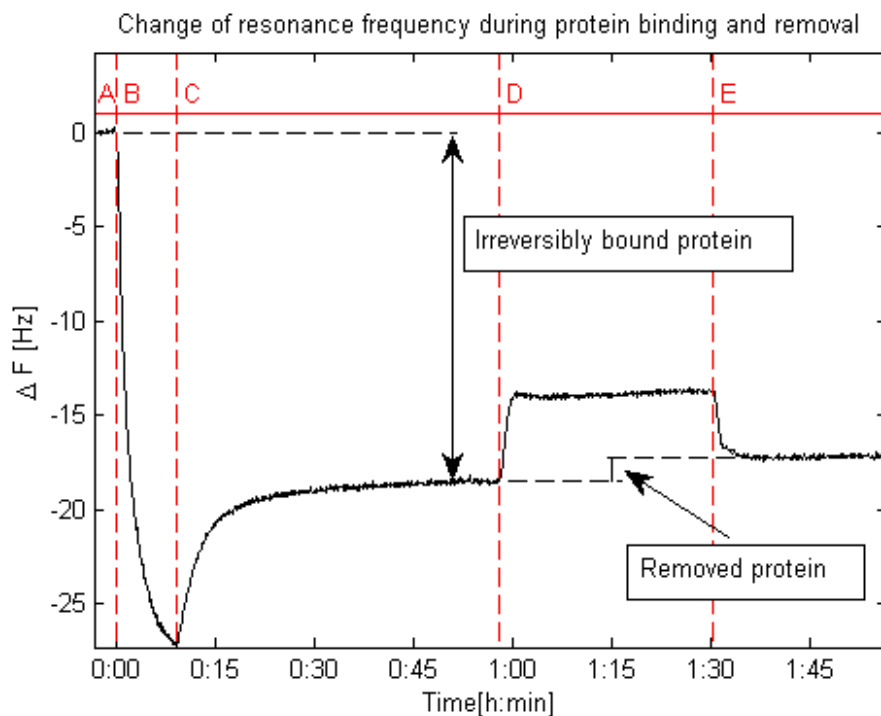


Figure 3.4: Resonance frequency shift (ΔF) as measured by QCM-D displaying the phases of a binding and dissolution experiment. Binding of the protein was done in buffer 4 (zone B). Dissolution was attempted by washing the protein bilayer with various buffers (e.g. buffers 1, 9, and 5) for ~ 30 min (zone D). Preceding and following these zones are rinses with buffer 4 (zones A, C, and E).

Irreversibly bound protein is defined as the difference in F before protein binding and after the rinsing of the protein has stabilised. Removed protein is defined as the difference in F before attempted dissolution and after the rinsing of the dissolution buffer has stabilised.

3.3 Microscopy

The microscope was used for two different types of measurements, Total Internal Reflection Fluorescence (TIRF) measurements and Surface Enhanced Ellipsometric Contrast (SEEC) measurements. Both measurements were performed with a Nikon 60x oil immersion objective (NA = 1.49), a CoolLED preciseExcite LED illumination system, and an Andor Neo sCMOS camera. The experiments were done in $15 \mu\text{l}$ PDMS wells temporarily attached to the substrate. The substrates were cleaned in boiling 7X detergent for 20 min, then rinsed with water, SDS, and water, and finally dried in a N_2 flow. The PDMS wells were cleaned in alcohol, rinsed with water, and dried in a N_2 flow.

3.3.1 Fluorescence microscopy

The basics of fluorescence microscopy are straightforward. A fluorophore is excited by a photon within a certain wavelength interval, it then relaxes from this state

by emitting a photon of lower energy i.e. longer wavelength. The light used for excitation can either be filtered to contain only the appropriate wavelengths for excitation or, as was the case during this thesis, a monochromatic light source can be used. To avoid various disturbances, mainly from non-absorbed excitation photons, the observed light is filtered to only contain photons in the emission region.

The fluorophore used in this thesis was nitrobenzoxadiazole (NBD) which has the maxima of its excitation spectrum at 460 nm and the maxima of its emission spectra at 534 nm. The light used for excitation came from an LED light and had its maxima at 465 nm. The filter cube used to separate these was a Nikon FITC cube.

Fluorescence Recovery After Photobleaching (FRAP) experiments were also performed to observe the mobility of the lipids within the bilayer. For these experiments a 40 mW, 475 nm laser, was used to photobleach the surface for 3 s.

3.3.2 Surface Enhanced Ellipsometric Contrast

Surface-enhanced ellipsometry contrast (SEEC) in combination with fluorescence imaging was used to observe the M1_C-induced clustering of DOPS. SEEC is a label-free imaging technique first described by Ausserré and Valingat in 2007 [38]. Its high spatial resolution and sensitivity was demonstrated by Gunnarsson et al. in 2012 [39] on protein binding to a heterogeneous SLB. The principle behind the technique is that linearly polarised light is used to illuminate the sample of interest, this changes the polarisation of the light and this change is measured as an output signal, see figure 3.5. The change in polarisation is affected by the change in total optical path length travelled, this in turn is affected by changes in distance travelled and the change in refractive index of the medium through which the light travels. To enhance the contrast of the resulting images a multi-layered anti-reflecting substrate is used, of which the top and bottom layers are SiO₂. Two linear polarisers are also needed for this technique, one to polarise the light before it reaches the sample and a second, at right angle to the first one, to remove the unchanged part of the signal.

3.3.3 Forming a supported lipid bilayer for the microscopy experiments

As was the case in QCM-D, lipid vesicles were used to form the SLB on the microscope. The composition of lipids used was 70/101 DOPC, 30/101 DOPS, 1/101 DOPS-NBD. Also, as in the QCM-D experiments, the lipid composition had a net negative charge and therefore Ca²⁺ ions were used as linking ions between the vesicles and the SiO₂ substrate (buffer 2, table 3.1).

To avoid photobleaching, SLB formation was not observed in real time. Fortunately, a well-formed SLB is easily distinguishable from the layer of lipid vesicles otherwise present. This can either be seen directly by increased strength and decreased smoothness of the fluorescence, as seen in figure 3.6, or in a more defined manner by performing a FRAP experiment. An SLB such as this, i.e. with no gel-phase components, should show recovery while a layer of vesicles should not.

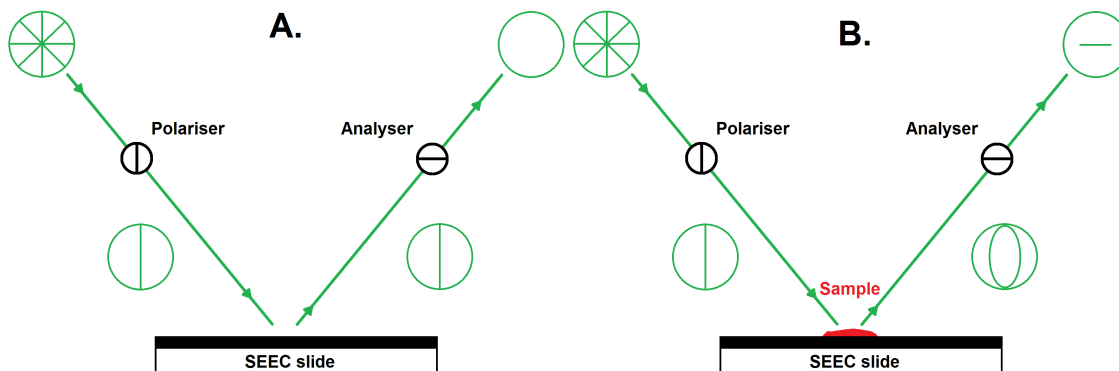


Figure 3.5: A schematic sketch of the principle behind Surface Enhanced Ellipsometric Contrast (SEEC). In A. linearly polarised light can be seen hitting the anti-reflecting SEEC slide, without changing its polarisation, and then be completely removed by the second linear polariser, denoted Analyser. In B. the light instead hits a sample which changes its polarisation slightly, this change is what is detected. These images are not completely representative for this thesis as the microscope used is inverted and therefore the light actually passes through the slide before hitting the sample.

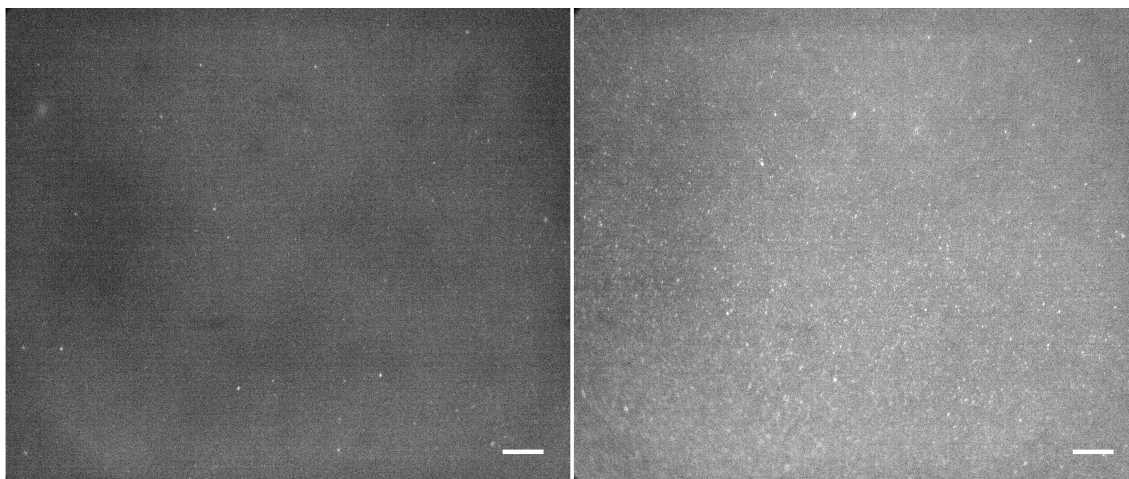


Figure 3.6: Total Internal Reflection Fluorescence (TIRF) microscopy images of an SLB (left), and a layer of lipid vesicles (right). As can be seen, the image of the SLB is less bright and more smooth than the image of lipid vesicles. The images were acquired under identical conditions and the same Lookup Table (LUT) has been used for both. Scale bar 20 μm .

3.3.4 Protein adsorption and dissolution on the microscope

The microscope was used to observe both full-length and N-terminal M1_C adsorbing to the SLB in a solution of 50 mM NaCl (buffer 4). Adsorption in different environments was not examined. The amount of protein used in these experiments were 150 ng, 15 μ l at 10 μ g/ml.

Dissolution of protein aggregates was attempted with 500 mM NaCl, pH 7.5 (1/1 mix of buffer 4 and buffer 9), and separately with 50 mM NaCl, pH 4.9 (buffer 5). These processes were periodically imaged and the experiments were stopped when no further changes were observed.

4

Results

In this chapter, the results from the QCM-D and microscopy experiments performed during this thesis are presented. In all experiments the binding of the M1_C protein to an SLB composed of DOPC (net neutrally charged) and DOPS (negatively charged), was investigated. The bilayer with adsorbed protein was then subjected to buffers with various properties, and its response was gauged. The chapter is divided into two parts: section 4.1 about the results from the QCM-D and section 4.2 about the microscopy results.

4.1 Quartz Crystal Microbalance with Dissipation monitoring

The QCM-D was used to observe and compare the binding behaviour of full-length and N-terminal M1_C, and to study protein layer dissolution upon exposure to different experimental conditions. A sample QCM-D curve including bilayer formation, binding and rinsing of the full-length protein in the standard environment (see section 3.2.3) can be seen in figure 4.1. This figure illustrates the typical QCM-D response for resonance frequency shift ΔF and dissipation shift ΔD during the different stages of the experiment. In this figure, the mass irreversibly bound can be seen at the end of zone H (see section 3.2.3 for the definition of irreversibly bound). When full-length M1_C was allowed to bind at 10 $\mu\text{g}/\text{ml}$, for ~ 10 min, the average mass irreversibly bound was 16.8 Hz ($\sigma=2.68$ Hz). The average mass irreversibly bound for N-terminal at 12 $\mu\text{g}/\text{ml}$, after ~ 12 min, was 10.0 Hz ($\sigma=3.30$ Hz).

To begin with, the binding behaviour upon rinsing with protein binding buffer (buffer 4) of full-length and N-terminal M1_C were compared. In both cases, a similar fraction of the proteins (70-80%) form irreversible bonds with the bilayer containing 30% DOPS (see section 3.2.3 for a definition of irreversibly bound). The rest forms reversible bonds and is subsequently rinsed off. In figure 4.2 two typical frequency data sets are plotted, showing the binding and rinsing of the proteins. The dissipation changes corresponding to these frequency changes are shown in figure 4.3. The kink in the full-length protein frequency plot after ~ 1 min is particularly interesting and is best illustrated in figure 4.4 in which ΔD is plotted against $-\Delta F$ in so called D-F plots. In figure 4.4, this kink can be seen as the part where ΔD has stabilised around $\sim 1.3 \cdot 10^{-6}$ but $-\Delta F$ keeps increasing from 15 Hz to 27 Hz. This indicates that the binding behaviour of the full-length protein has two distinct regimes. The N-terminal on the other hand has an approximately linear behaviour throughout binding. However, upon rinsing, the full-length protein seems to exhibit

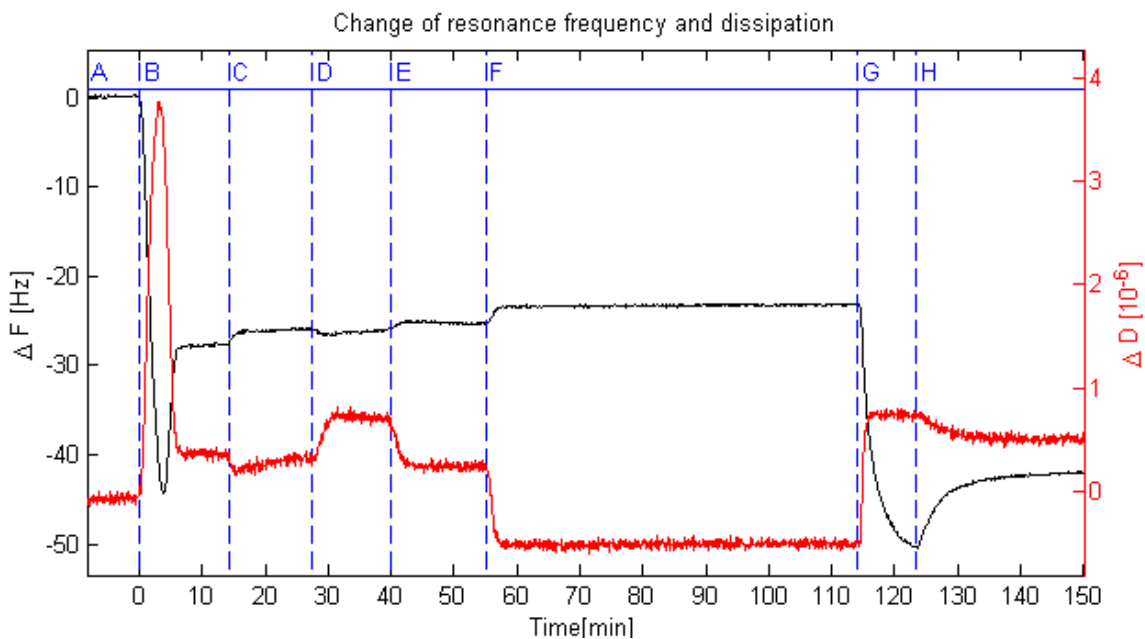


Figure 4.1: QCM-D data of SLB formation and binding and release of full-length protein. Bilayer formation (zone B, buffer 2 + lipids) and ethylenediaminetetraacetic acid (EDTA) wash (zone D, buffer 3) are both preceded and followed by rinses (zones A, C, and E, buffer 1). The protein binding (zone G, buffer 4 + protein) is preceded and followed by rinses (zones F and H, buffer 4). See sections 3.2.2 and 3.2.3 for details on proteins and lipids, and see table 3.1 for details on the buffers.

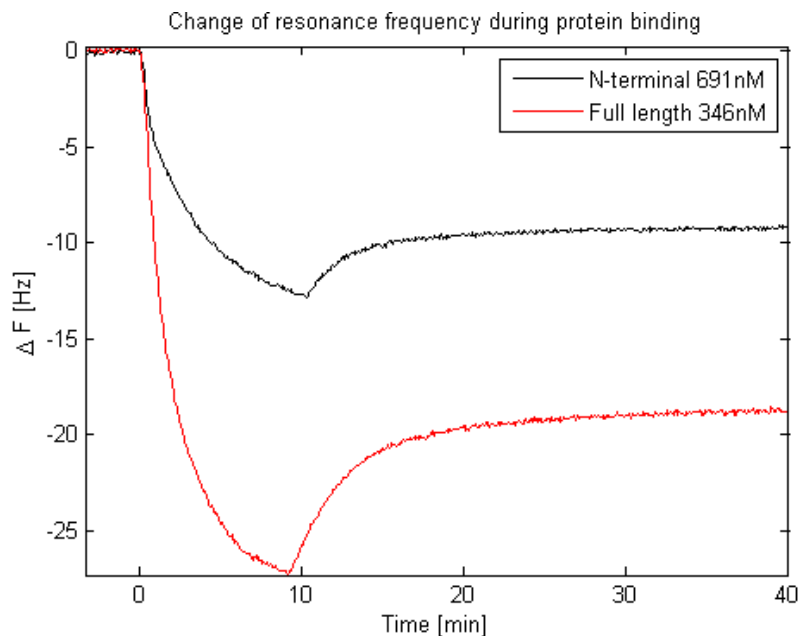


Figure 4.2: Change of frequency as measured with QCM-D of full-length (red curve) and N-terminal (black curve) $M1_C$ binding and releasing in the standard conditions. A significant and similar portion of the protein is irreversibly bound. For a definition of irreversibly bound see figure 3.4.

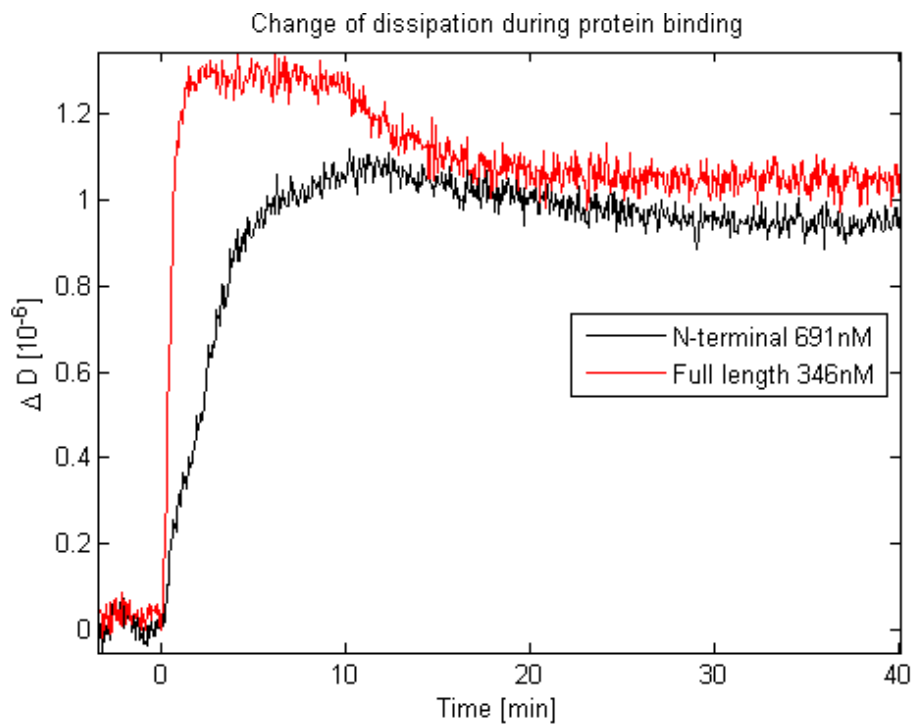


Figure 4.3: Change of dissipation as measured with QCM-D while binding and rinsing full-length and N-terminal $M1_C$. These measurements are from the same data set as the plots in figure 4.2.

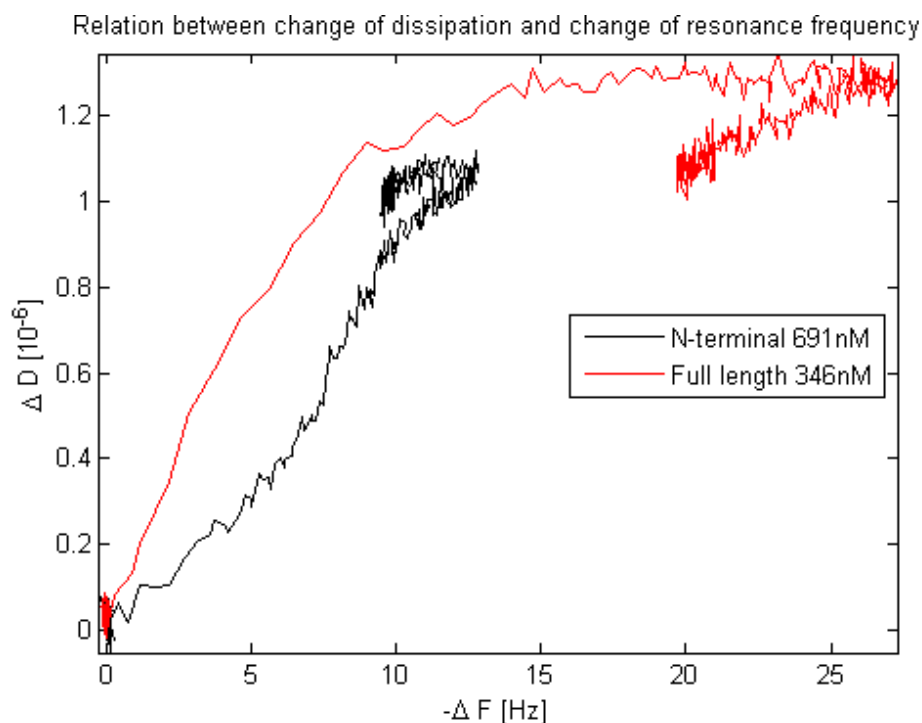


Figure 4.4: D - F plots of the two data sets from figures 4.2 and 4.3. These illustrate the difference between the full-length and the N-terminal protein in the binding process.

a linear $-\Delta F$ vs ΔD behaviour while the N-terminal seems to lose mass without the dissipation decreasing. In some N-terminal cases this has been even more unintuitive showing the crystal losing mass while gaining dissipation. This could be due to the fact that some proteins detach from the bilayer (loss in mass), and others reorganise into less rigid structures (increased dissipation), either as individual proteins or as aggregates. The ratio $\frac{\Delta D}{-\Delta F}$ at the stable endpoints is on average twice as high for N-terminal compared to full-length protein. A higher dissipation per mass means that the proteins rigidity is lowered, through structural changes in each protein or in the aggregates of proteins. For a collection of N-terminal D-F plots, see figure A.1 in appendix A.

4.1.1 Initial binding is charge dependent

Two experiments were done to examine if the initial binding of the full-length protein is dependent on electrostatic charges. The first experiment consisted in letting the protein bind to a bilayer containing 100 % DOPC. This was done to examine whether removing the negative charge from the bilayer would prevent protein binding. The second experiment was to increase the amount of NaCl in the buffer surrounding the proteins during binding. This was done to examine whether electrostatically screening the proteins would hinder binding. The concentration of NaCl was increased from 50 mM to 150 mM. The results of both experiments can be seen in figure 4.5. As can be seen, the full-length protein binding was undetectable when faced with the bilayer lacking negative charges.

The binding behaviour of full-length and N-terminal M1_C was compared in standard and elevated NaCl concentrations. The average mass of full-length protein irreversibly bound was decreased by 96 % (from 16.8 Hz to 1.0 Hz) when the concentration of NaCl was increased. The average amount of N-terminal irreversibly bound in the increased NaCl concentration was <1 Hz, making the decrease at least 90 % (from 10.0 Hz to <1 Hz). In conclusion, the binding of both versions of the protein is highly dependent on the concentration of ions in the surrounding buffer.

4.1.2 Attempted protein layer dissolution

Since dissociation of M1 from the the lipid envelope of the virion is regarded as a vital part of the infection cycle, the dissolution of the protein layer in different environments was examined. As an increased concentration of NaCl greatly inhibited the binding of the protein, it was deemed interesting to gain further insights into the contribution of electrostatics. This was done by choosing an increased concentration of NaCl as one of the removal strategies. The other chosen strategy was low pH, this was chosen since a low pH has been shown to affect several aspects of the behaviour of M1 from influenza A and in particular to increase its tendency to dissociate from the lipid bilayer (for details see section 2.2).

Removal experiments were performed by exchanging the standard buffer (50 mM NaCl, pH 7.5, buffer 4) with the chosen removal buffer for 30 min, see figure 3.4. The first NaCl concentration tried was 150 mM (pH 7.5, buffer 1), as this was the same used in the binding experiments. As can be seen in figure 4.6 and table

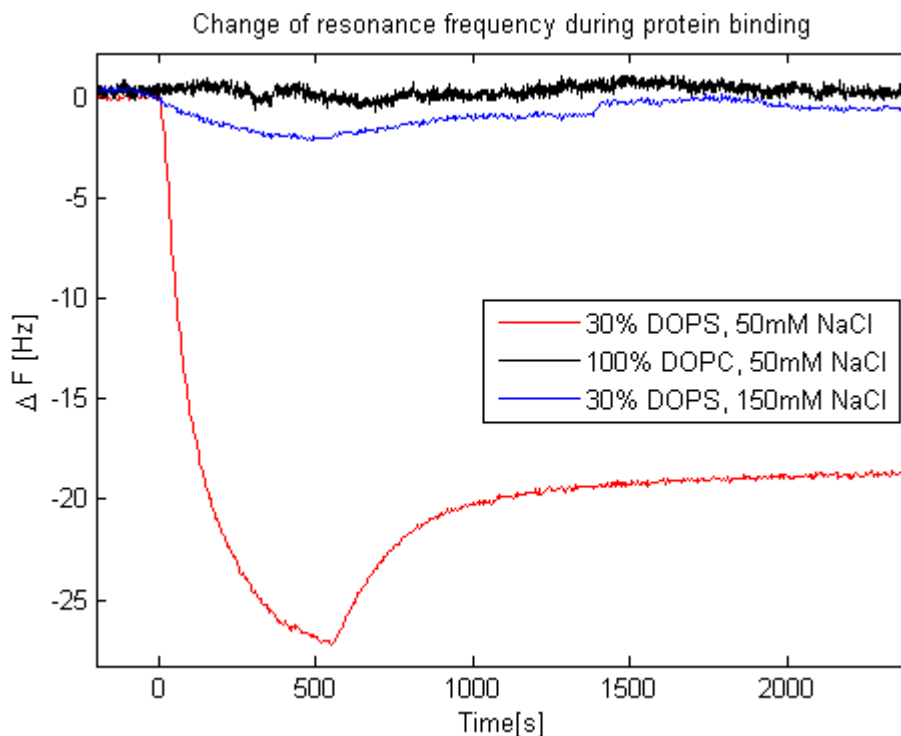


Figure 4.5: Change of frequency as measured with QCM-D for the binding and release of full-length $M1_C$ in different environments. These environments are: a bilayer containing 30 % 1,2-dioleoyl-*sn*-glycero-3-phospho-*L*-serine (DOPS) in a buffer with 50 mM NaCl (red curve, buffer 4) or 150 mM NaCl (blue curve, buffer 1), or a bilayer containing 100 % 1,2-dioleoyl-*sn*-glycero-3-phosphocholine (DOPC) in 50 mM NaCl buffer (black curve, buffer 4).

4.1 this partially removed both kinds of protein. As an alternative to NaCl, KCl was used at 150 mM, this did not generate results significantly different from the ones found with NaCl (data not shown), more rigorous experiments with KCl were not performed. To examine if the removal effect could be enhanced by increasing the NaCl concentration, another series of removals were tried using 950 mM NaCl (pH 7.5, buffer 9). As can be seen in the previously referenced figure and table, this did indeed enhance the removal effect. The effect was less pronounced in the attempted removals with buffer at pH 4.9 (50 mM NaCl, buffer 5). The common tendency for all three strategies is that the N-terminal protein is more easily removed than the full-length protein. To examine if the amount of protein removed was dependent on the time it was exposed to the removal buffer, both longer exposure times and repeated exposures were tested. Neither increased the amount of protein removed (data not shown), this indicates that 30 minutes is enough to reach the maximum removal for the buffers tested.

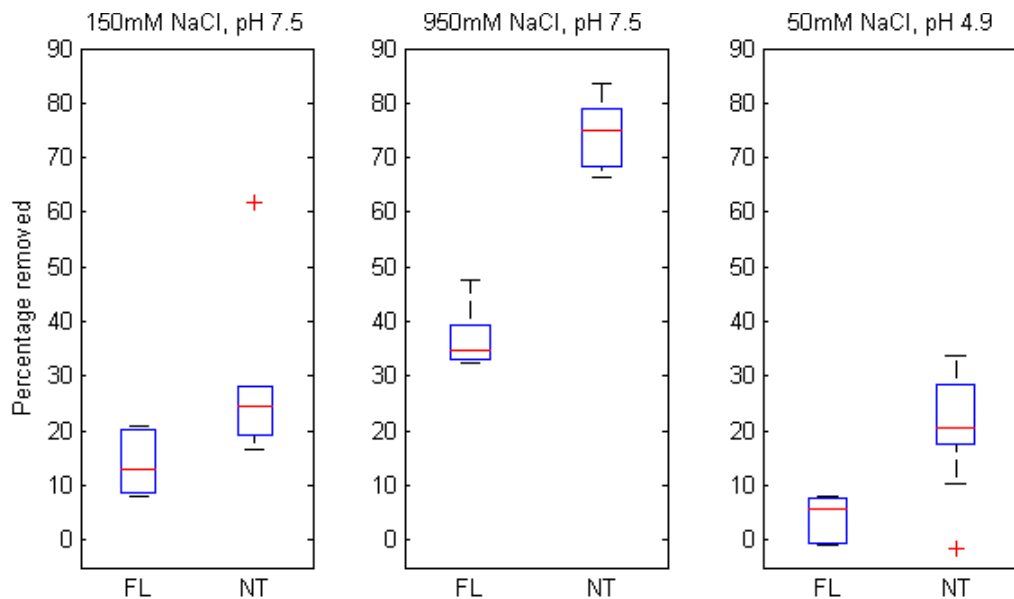


Figure 4.6: Box plots of the percentage of the irreversibly bound protein that was removed by changing the properties of the surrounding buffer for 30 min. All proteins were bound at 50 mM NaCl, pH 7.5 (buffer 4). The box plots in the left and centre graphs shows the reaction to an increased ion concentration. In the left graph, the concentration of NaCl was increased to 150 mM (buffer 1), in the centre graph to 950 mM (buffer 9). The box plots in the right graph shows the reaction to lowering the pH to 4.9 (buffer 5).

Removal	150 mM, pH 7.5		950 mM, pH 7.5		50mM, pH 4.9	
	Mean	σ	Mean	σ	Mean	σ
full-length	13.93 %	5.73 %	36.98 %	5.37 %	4.17 %	4.02 %
N-terminal	29.15 %	16.45 %	74.55 %	6.51 %	20.50 %	10.72 %

Table 4.1: Mean percentages and standard deviations (σ) of the removal of irreversibly bound proteins by changing the surrounding buffer for 30 min. The data set is the same that was used for figure 4.6. The three different buffers with which removal was attempted were: 50 mM NaCl at pH 4.9 (buffer 5), 150 mM NaCl at pH 7.5 (buffer 1), and 950 mM NaCl at pH 7.5 (buffer 9). Each statistic was calculated from a minimum of six experiments each.

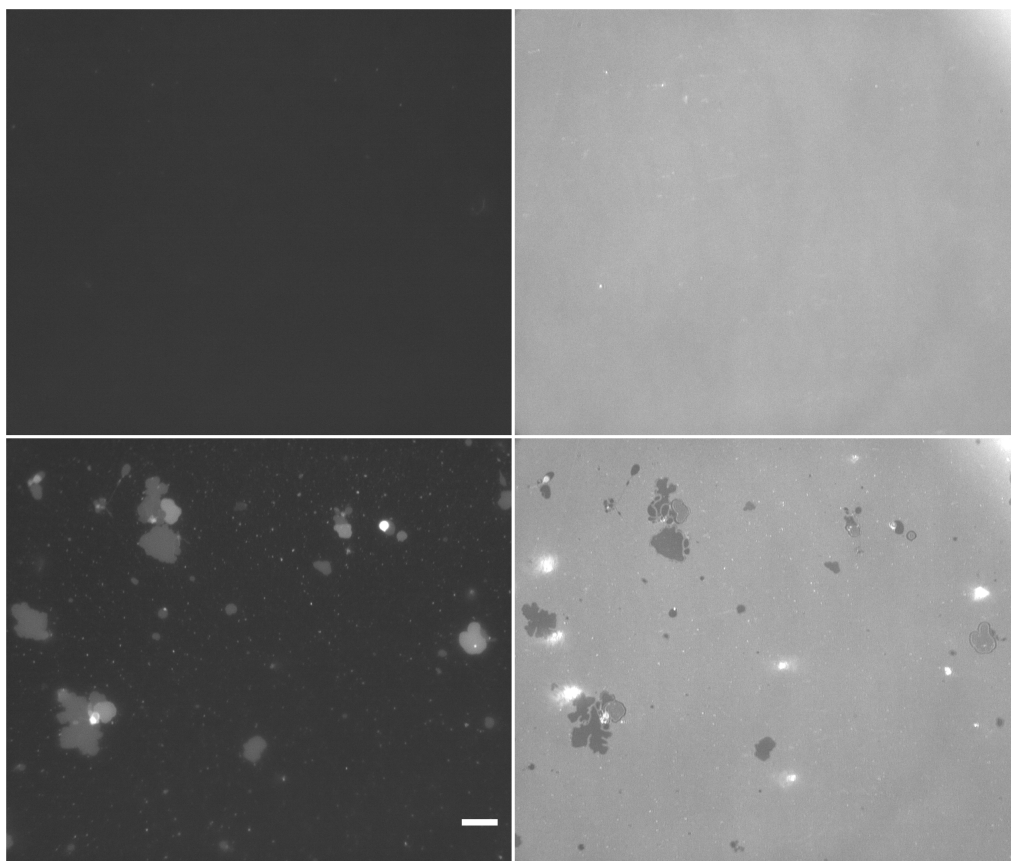


Figure 4.7: *TIRF and SEEC microscopy images taken before and after adsorption of N-terminal protein. The upper images were taken before protein adsorption and the images below were taken after. The images on the left were taken with TIRF microscopy and the images on the right were taken with SEEC microscopy. The areas of increased fluorescence intensity seen in the lower left image correlates very well with the areas of increased thickness seen in the lower right image. Scale bar 19.5 μm .*

4.2 Fluorescence microscopy & Surface Enhanced Ellipsometric Contrast (SEEC) microscopy

The spatial behaviour of full-length and N-terminal $M1_C$ aggregates was observed with two different microscopy techniques in different environments. The two techniques used were TIRF microscopy and SEEC microscopy. The first was used to observe fluorescently tagged DOPS to which $M1_C$ binds according to the previously shown QCM-D data. The SEEC on the other hand was used to image the thickness of the different regions on the SLB and hence to visualise the protein adlayer which produces darker signals (see section 3.3.2 for details on how this is done).

The microscopy data further confirms that the protein binds to the SLBs and also reveals that it has a tendency to form aggregates. As can be seen in figure 4.7, the presence of clusters of fluorescently tagged lipids seen in the TIRF microscopy correlates very well with the areas of changed thickness seen in the SEEC microscopy.

4. Results

For the rest of the report, both these types of areas will be assumed to correspond to protein aggregates. The clusters have varying morphologies, from clusters of indistinct shapes to lines or tubes, and diameters ranging from a few μm (close to the resolution of the microscope) to $20\ \mu\text{m}$. Examples of these can be seen in figures 4.8 and 4.9. No statistically significant difference was found between the aggregation patterns of full-length and N-terminal $M1_C$. There was however a weak tendency for the full-length protein to form larger aggregations.

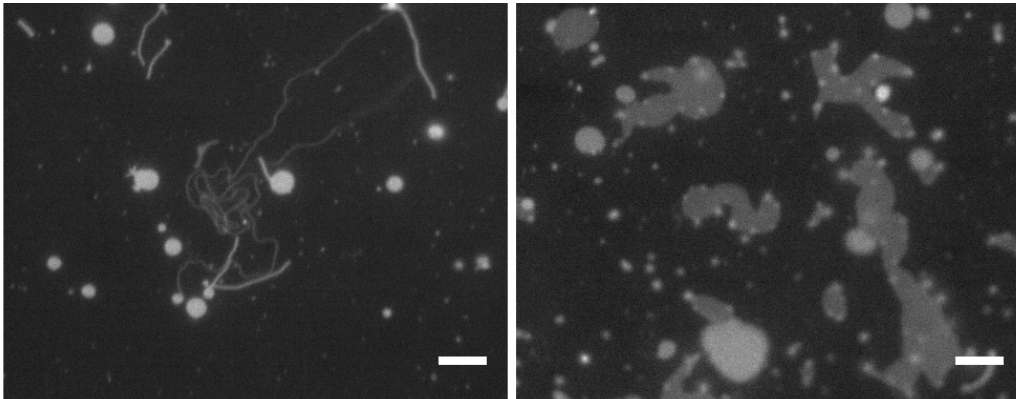


Figure 4.8: *TIRF microscopy images of full-length protein aggregates. Two variants of aggregation can be seen: line-like aggregations, and small to large sized aggregates. Scale bars $10\ \mu\text{m}$.*

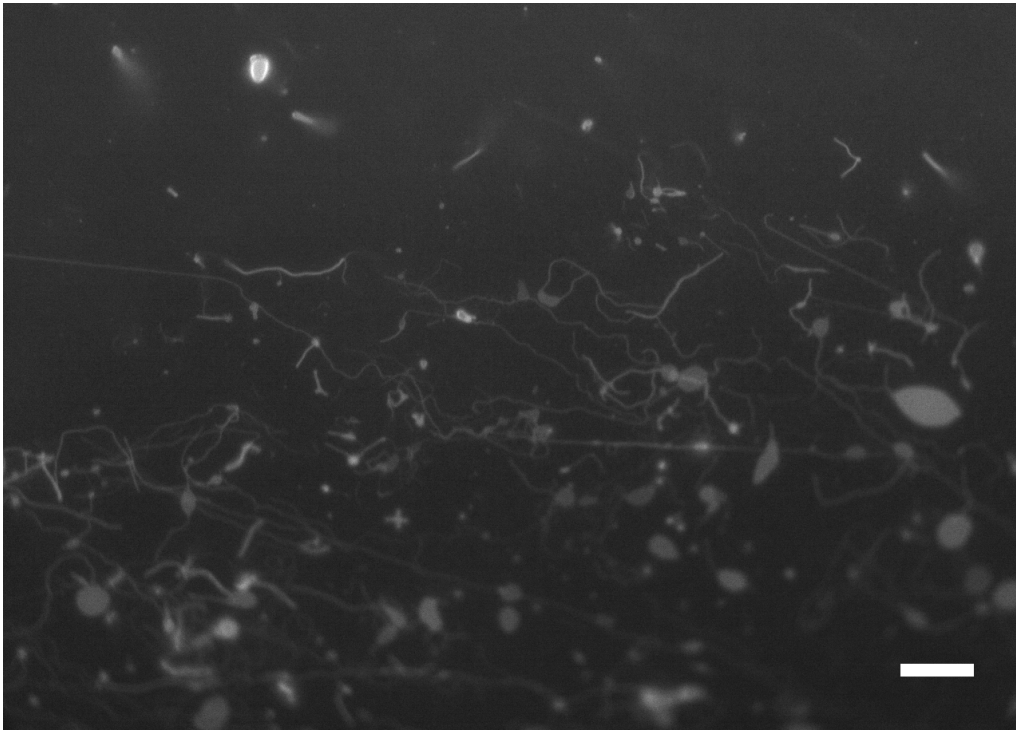


Figure 4.9: *TIRF microscopy image of N-terminal protein aggregates. Three variants of aggregation can be seen: no aggregation, linelike aggregations, and small to moderately sized aggregates. Scale bar $20\ \mu\text{m}$.*

4.2.1 Externally induced changes on protein aggregate morphology

In the first part of this chapter it was shown that the irreversibly bound protein is sensitive to drastic changes in the surrounding environment. The two changes investigated were increased NaCl concentration and lowered pH.

In the QCM-D experiments, it was found that part of the proteins were removed from the SLB by increasing the concentration of NaCl in the surrounding buffer, this finding was supported by the microscopy observations. The protein aggregates gradually dissipated when exposed to 500 mM NaCl, pH 7.5. In the microscope it is not possible to tell if the proteins have dissociated from the SLB completely or are still adsorbed but have dissociated from the protein aggregates. Whether the proteins detached from the SLB and released the cluster of lipids bound by them or the proteins detached from each other and the resulting clusters of lipids were too small to observe was not investigated. However, if the latter was the case this would not register in the QCM-D since the mass coupled to the crystal would be essentially unchanged. An additional facet of the behaviour was also observed in this experiment. Different clusters started dissipating both at different times and at different speeds. These results were similar in both full-length and N-terminal M1_C see figures 4.10 and 4.11 respectively.

In the QCM-D experiments (figure 4.6), it was shown that exposing full-length M1_C to a buffer with 50 mM NaCl and pH 4.9 for 30 min had a very small effect, if any. The same kind of experiment was observed for full-length M1_C with TIRF microscopy. Here the effect seems more distinct. Protein aggregates seemed to shrink in the low pH environment, see figure 4.12. This, in combination with the result from the QCM-D, could indicate that the low-pH environment weakens the protein-protein bonds but not protein-SLB bonds in which case the proteins are still attached to the bilayer but do not form aggregates. Unfortunately this experiment was never successfully performed with N-terminal protein.

4.2.2 Diffusive behaviour of DOPS

To examine whether M1_C immobilises the lipids it attaches to, an experiment was done where DOPS both inside and outside clusters was photobleached. As can be seen in figure 4.13, the clusters are recovering after photobleaching and can therefore not be completely immobilised by the proteins. The diffusion constants of the bilayer was not measured therefore it has not been determined whether the protein clusters partially hinder the diffusion of the lipids.

Since the continuous observation of the fluorescently tagged lipids bleaches the attached fluorophore it was deemed a necessary control to observe the reaction of the SLB and protein to this process. The results can be seen in figure 4.14. As can be seen, the fluorescence is mostly bleached away while the SEEC image seems completely unaffected. It is therefore concluded that the unavoidable photobleaching of the NBD attached to some DOPS does not affect the behaviour of the protein. Since the NBD is located in the hydrophobic inner of the SLB this is what could be expected.

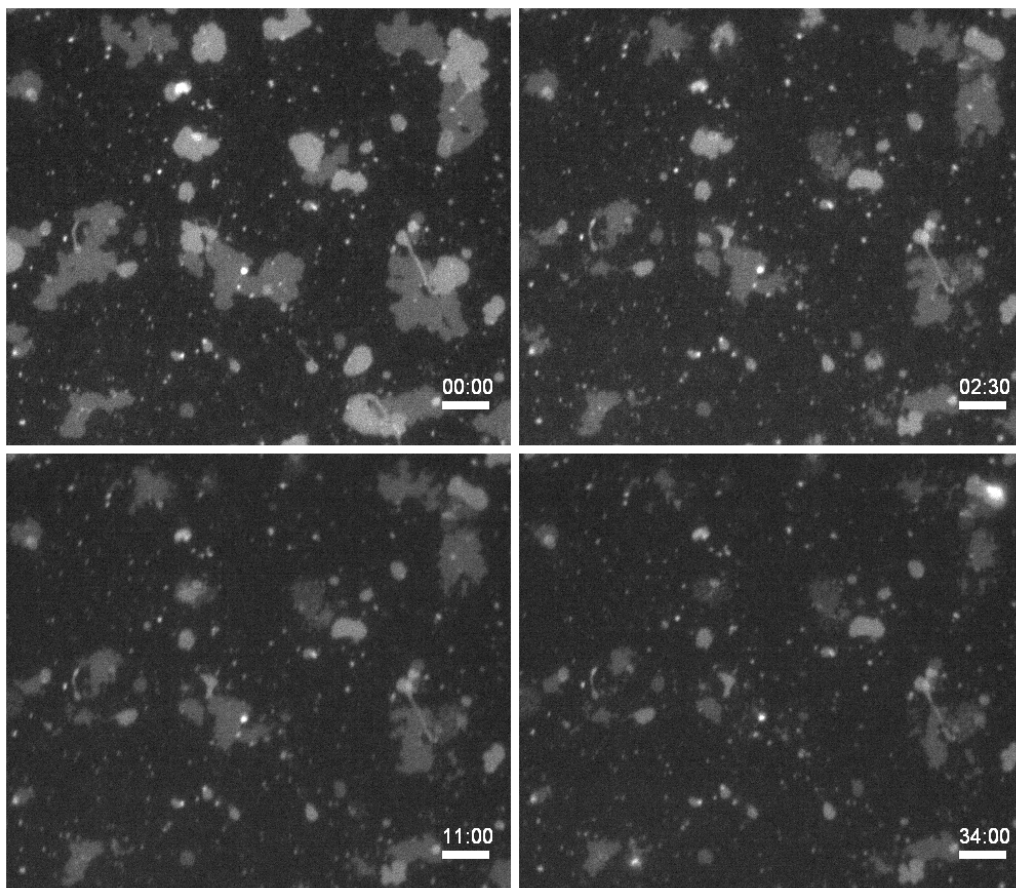


Figure 4.10: *TIRF images of full-length protein aggregations observed while reacting to a buffer change from 50 mM NaCl, pH 7.5 (buffer 4) to 500 mM NaCl, pH 7.5 (1/1 mix of buffer 4 and buffer 9). Upper left is at change of buffer. Upper right is 150 s later. Lower left and right are 11 min and 34 min respectively after change of buffer. As can be seen some aggregations are dissolved very quickly (2.5 min), some are unaffected for a moderate amount of time (11 min) but are then dissolved, and some aggregations, and parts of aggregations, are not affected at all before the end of the observation (34 min). Scale bars 10 μ m.*

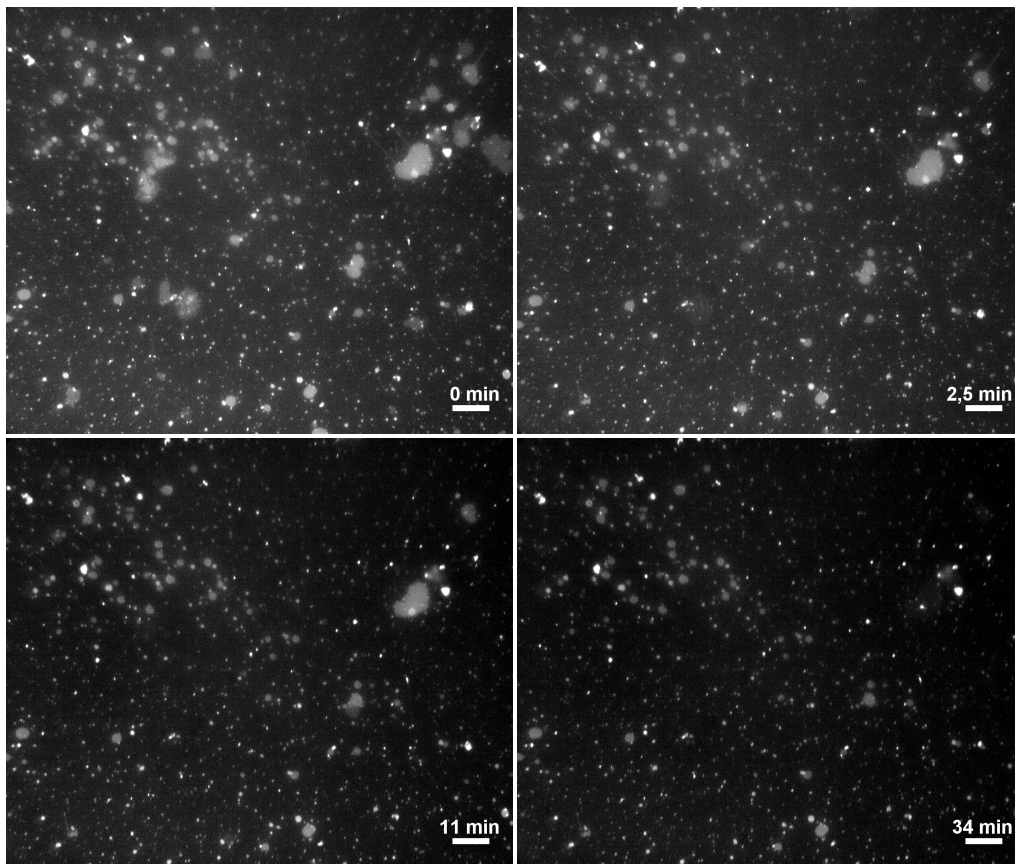


Figure 4.11: *TIRF images of N-terminal protein aggregations observed while reacting to a buffer change from 50 mM NaCl, pH 7.5 (buffer 4) to 500 mM NaCl, pH 7.5 (1/1 mix of buffer 4 and buffer 9). Upper left is at change of buffer. Upper right is 150 s later. Lower left and right are 11 min and 34 min respectively after change of buffer. As can be seen some aggregations are dissolved very quickly (2.5 min), some are unaffected for a moderate amount of time (11 min) but are then dissolved, and some aggregations, and parts of aggregations, are not affected at all before the end of the observation (34 min). Scale bar 20 μ m.*

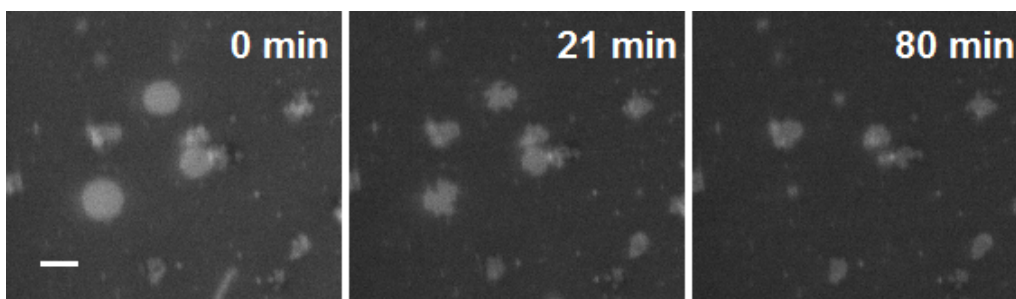


Figure 4.12: *TIRF images of full-length M1C being exposed to pH 4.9. Images taken, from left to right, after 0, 21, and 80 min. Some regions seem to disappear completely while others seem largely unaffected. Scale bar 4.55 μ m.*

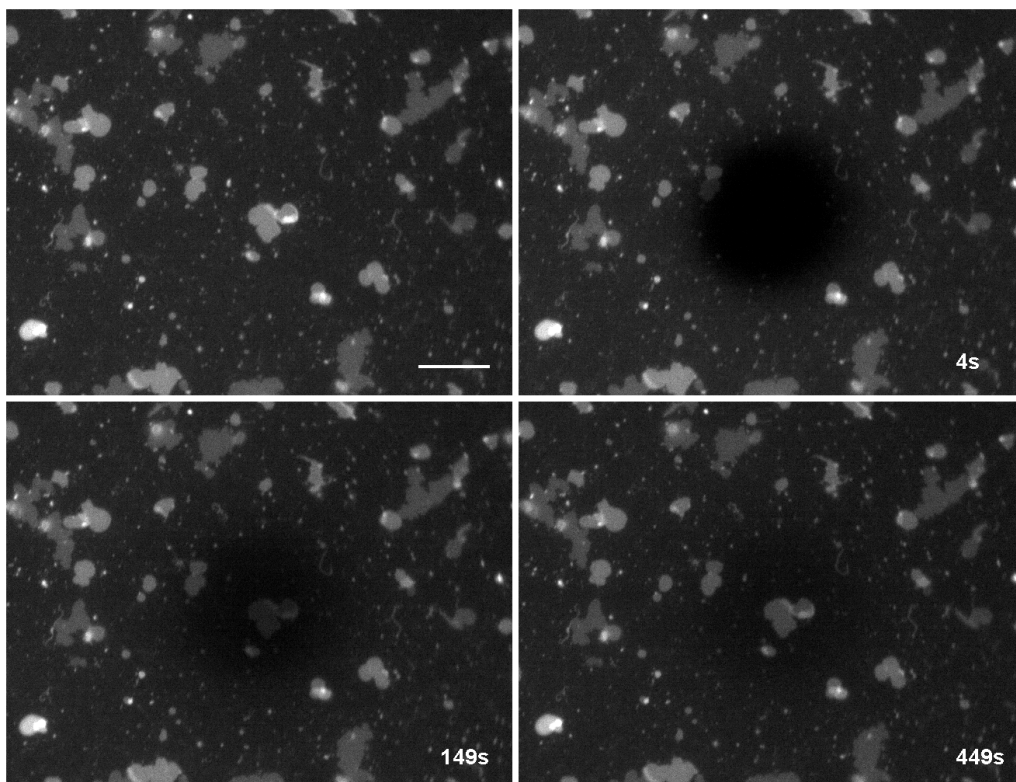


Figure 4.13: *Fluorescence images of a photobleached lipid bilayer containing fluorescently labelled DOPS (DOPS-NBD) and with adlayered full-length protein clusters. As established earlier, these protein clusters coincide with the areas of higher concentrations of DOPS-NBD seen in images. The upper right image was taken before photobleaching, on the other images the times since photobleaching are given. As can be seen, both the bilayer and the clusters recover over time. Scale bar 20 μm .*

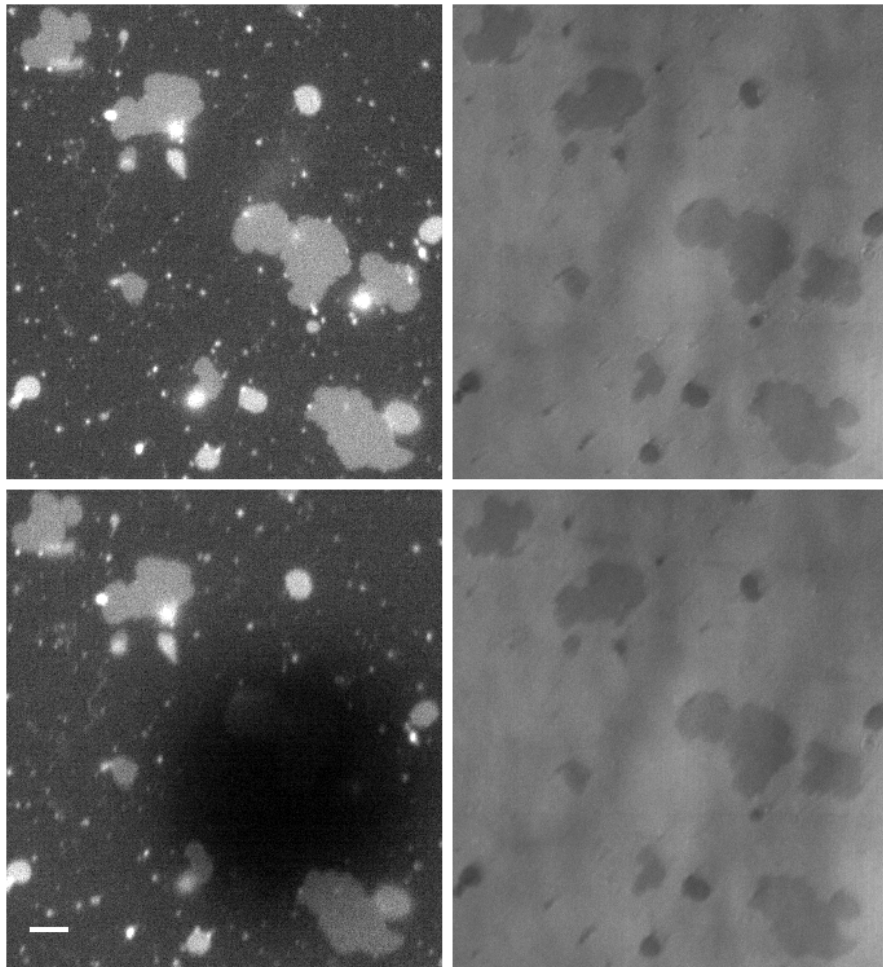


Figure 4.14: *TIRF and SEEC images of a photobleached bilayer containing DOPS-NBD and with adlayered protein clusters. The TIRF images on the left show the photobleaching of the fluorophore. In the SEEC images on the right no response to the treatment can be seen. Scale bar 6.5 μm .*

5

Discussion

In this chapter, the findings from chapter 4, Results, are examined and the origins of the found behaviours are speculated upon. The findings are also compared to previously published results, mainly concerning influenza A. Finally, future prospects and projects are suggested.

5.1 Protein binding

The lipid binding properties of $M1_C$ are interesting because of the proteins proximity to the lipid envelope of the virion. The binding of full-length and N-terminal protein was examined by QCM-D and a combination of fluorescence and SEEC microscopy. The protein was found to bind to negatively charged lipids and form aggregates on the SLB. Some differences were found between full-length and N-terminal, particularly in their QCM-D dissipation profiles during binding.

5.1.1 Protein-lipid binding

Both the results from the QCM-D and the microscopy show that both full-length and N-terminal $M1_C$ bind to an SLB, with at least part of this binding being irreversible (figures 4.2, 4.7, and 4.8). The SLB used contained DOPS which shows that $M1_C$, akin to $M1_A$, can bind to bilayers containing negatively charged lipids [6, 10]. Further, $M1_C$ seems to require negatively charged lipids for binding (figure 4.5, red curve compared to black curve), this behaviour differs from that of $M1_A$ which seems to benefit from, but not require them [9]. The N-terminal also binds to a negatively charged SLB which is in accordance to the results from influenza A [6]. These behaviours makes it probable that the protein-lipid binding is partially, or at least initially, electrostatic in nature. The other result shown in figure 4.5 shows that the initial binding of $M1_C$ can be heavily impeded by increasing the ion content of the surrounding buffer. Since increased ion content leads to increased electrostatic screening this result lends further credence to the theory that the initial protein-lipid binding is mainly electrostatic.

Since the proteins bind mainly to negatively charged lipids, a subsequent question was whether these lipids were immobilised by the proteins. As can be seen in figure 4.13 this was not the case. Since the clusters recovered after bleaching the bleached lipids must have been replaced by unbleached ones which shows that the lipids are still mobile.

5.1.2 Aggregation

Since the mutual interaction between $M1_A$ proteins has been indicated as an important aspect of the proteins role, particularly in determining the morphology of the virion [8], the study of the aggregation of the protein was deemed worthwhile. As can be seen in figures 4.7, 4.8, and 4.9 both full-length and N-terminal $M1_C$ aggregates on SLBs. For full-length $M1_C$, these results have been seen previously [25]. This has also been shown previously in influenza A by Hilsch et al. [9], who also showed that $M1_A$ did not aggregate in solution, only in close proximity to the lipid bilayer.

The results from this thesis also show that the N-terminal retains the full-length proteins tendency to oligomerise. In influenza A it has been shown that the N-terminal is responsible for oligomerisation of orders greater than two [12]. Since it aggregates in the experiments performed in this thesis the N-terminal protein must retain at least some of the oligomerisation capabilities of the full-length protein.

5.1.3 QCM-D dissipation changes during binding

The change of dissipation during binding for full-length and N-terminal protein showed apparent differences (figures 4.3 and 4.4). Since the frequency binding curves look very similar (figure 4.2) this is probably not a change in the protein-lipid interactions but should rather be related to protein-protein interactions or protein layer structure. In the first part of figure 4.4 (from the origin until $-\Delta F \approx 12$ Hz), the dissipation increases more per mass for full-length than for N-terminal. This could be an effect of differing protein structures, if N-terminal has a tighter structure than full-length it would couple less water per mass and therefore impose a smaller dissipation change per mass. Another reason for this effect could be that the N-terminal has a larger part inserted into the membrane and therefore couples less water per mass. The last part of figure 4.4 (from the points on the graphs where mass starts decreasing until the end) however, displays the opposite outcome: At the end of the graphs, where the experiment has stabilised, the full-length protein has about half the dissipation change per mass. This means that in the end the full-length protein layer must have a tighter structure than that of the N-terminal, this structure must therefore change during the binding. This change could be either a tightening of the individual proteins, a tightening of the oligomer structure of the proteins, or an insertion of the proteins into the lipid bilayer. This change, whichever it is, should be caused by the crowding of the proteins since this factor is the only one changing during the experiment.

5.2 Dissociation

Since it has been shown that the dissociation of $M1_A$ from the lipid envelope of the virion is a critical part of the infection [40] this dissociation was examined both by QCM-D and microscopy. In the QCM-D, a change in resonance frequency can be directly correlated to a change in the amount of protein bound to the SLB. However, no such conclusion can be drawn from the microscopy results. The disappearance

of the distinguishable DOPS-NBD clusters in the microscopy experiments is not necessarily caused by the dissociation of $M1_C$ from the SLB. Another reason for their disappearance could be that $M1_C$ proteins dissociates from each other and the DOPS-NBD clusters bound by a single protein are too small to be detectable in the microscope.

5.2.1 Charge-dependent dissociation

The QCM-D results shown in figure 4.6 (left and centre graphs) and table 4.1 shows dissociation of irreversibly bound full-length and N-terminal protein by increased ion content. This dissociation strategy was repeated in the microscope (figures 4.10 and 4.11) with similar results. This indicates that electrostatics are important not only initially but also plays a role in the persistent binding between proteins and lipids. However, since not even 950 mM NaCl could remove all of the protein, irrespective of exposure time, there must be some other mechanism protecting the protein from this kind of removal. This could be due to either a non-electrostatic binding between $M1_C$ and SLB or some structural arrangement that protects the binding sites from the influence of the ions in the surrounding buffer.

5.2.2 pH-dependent dissociation

Since the acidification that takes place in the endosomes during virion entry has been found to be a crucial part in the spreading of the virus [17], the influence of pH on the $M1$ layer integrity was considered worthwhile examining. Dissociation was therefore attempted by lowering the pH of the buffer surrounding the proteins and the SLB. The results (shown in figures 4.6 and 4.12, and table 4.1) were that there was a dissociation but it was less pronounced than what was seen in the experiments with increased ion content. The disassociation of $M1_A$ from a lipid bilayer by low pH has been studied before by Fontana et al. [28]. However, the results are difficult to compare with the results of this thesis since the experiments were performed on complete virions and expressed the disassociation as the percentage of virions that had lost their resolved $M1_A$ layer after exposure to low pH, these experiments were done with cryo-electron tomography. Fontana et al. classified all virions as either possessing or not possessing a resolved bilayer and this distinction was done by visual inspection. Our results are in little agreement with the idea that the dissolution of the protein lining on the inside of the virions is an integral process in the uncoating of the protein [41]. A variation on the uncoating process has been proposed where the $M1_A$ layer breaks down after the lipid bilayers of the virion and the endosome have already fused [42]. If this is true, the break down of the protein layer could be highly dependent on mechanical stress. This is a potential reason for the observed discrepancies since the mechanical stress was not present in the experiments of this thesis. However, this still does not account for the differences to Fontana et al., since the mechanical stress was not present in their experiments either.

5.3 Future research

As was written in section 3.2.3 the QCM-D experiments in this thesis were all performed with a set amount of protein. The reason for this was mostly to conserve protein reserves. As can be seen in figure 4.2, this amount was not enough to saturate the binding process. Whether this affects the amount of irreversibly bound protein was not examined.

Utilising Surface Resonance Plasmon (SPR) Brevnov et al. [27] have shown that initial binding rate, average binding rate, irreversibility of binding, and saturated level of adsorption of $M1_A$ all depend on the pH at which the protein was bound. Performing these studies on $M1_C$ would enable interesting comparisons between the two proteins.

On a grander scale, it is highly unlikely that influenza C will be eradicated in the foreseeable future. This is not because it would be virtually impossible as with influenza A and B, which have frequent and significant mutations. Rather because the gains of preventing some cases with cold-like symptoms and a minuscule number of more severe cases would not match the expenses associated with eradicating the disease.

Bibliography

- [1] World Health Organization. *Influenza (Seasonal) Fact sheet N°211*. [Online]. <http://www.who.int/mediacentre/factsheets/fs211/en/>. Mar. (2014).
- [2] Centers for Disease Control and Prevention. “Influenza”. In: *Epidemiology and Prevention of Vaccine-Preventable Diseases*. Ed. by Hamborsky J, Kroger A, Wolfe S. 13th. Washington DC: Public Health Foundation, (2015). Chap. 12.
- [3] A. Joosting et al. “Production of common colds in human volunteers by influenza C virus”. In: *British medical journal* 4.5624 (1968), p. 153.
- [4] Y. Matsuzaki et al. “Clinical features of influenza C virus infection in children”. In: *Journal of Infectious Diseases* 193.9 (2006), pp. 1229–1235.
- [5] M. Yamashita, M Krystal, and P. Palese. “Evidence that the matrix protein of influenza C virus is coded for by a spliced mRNA”. In: *Journal of virology* 62.9 (1988), pp. 3348–3355.
- [6] F. Baudin et al. “In vitro dissection of the membrane and RNP binding activities of influenza virus M1 protein”. In: *Virology* 281.1 (2001), pp. 102–108.
- [7] A. Ali et al. “Influenza virus assembly: effect of influenza virus glycoproteins on the membrane association of M1 protein”. In: *Journal of virology* 74.18 (2000), pp. 8709–8719.
- [8] D. P. Nayak et al. “Influenza virus morphogenesis and budding”. In: *Virus research* 143.2 (2009), pp. 147–161.
- [9] M. Hilsch et al. “Influenza A Matrix Protein M1 Multimerizes upon Binding to Lipid Membranes”. In: *Biophysical journal* 107.4 (2014), pp. 912–923.
- [10] R. W. Ruigrok et al. “Membrane interaction of influenza virus M1 protein”. In: *Virology* 267.2 (2000), pp. 289–298.
- [11] J. Fontana and A. C. Steven. “At low pH, influenza virus matrix protein M1 undergoes a conformational change prior to dissociating from the membrane”. In: *Journal of virology* 87.10 (2013), pp. 5621–5628.
- [12] K. Zhang et al. “Dissection of influenza A virus M1 protein: pH-dependent oligomerization of N-terminal domain and dimerization of C-terminal domain”. In: *PloS one* 7.5 (2012), e37786.
- [13] G Herrler et al. “The glycoprotein of influenza C virus is the haemagglutinin, esterase and fusion factor.” In: *The Journal of general virology* 69 (1988), pp. 839–846.

- [14] M. von Itzstein. “The war against influenza: discovery and development of sialidase inhibitors”. In: *Nature reviews Drug discovery* 6.12 (2007), pp. 967–974.
- [15] A. Pekosz and R. A. Lamb. “The CM2 Protein of Influenza C Virus Is an Oligomeric Integral Membrane Glycoprotein Structurally Analogous to Influenza A Virus M2 and Influenza B Virus NP Proteins”. In: *Virology* 237.2 (1997), pp. 439–451.
- [16] T. Betakova and A. J. Hay. “Evidence that the CM2 protein of influenza C virus can modify the pH of the exocytic pathway of transfected cells”. In: *Journal of general virology* 88.8 (2007), pp. 2291–2296.
- [17] S. Li et al. “pH-controlled two-step uncoating of Influenza virus”. In: *Biophysical journal* 106.7 (2014), pp. 1447–1456.
- [18] M. Bui, G. Whittaker, and A. Helenius. “Effect of M1 protein and low pH on nuclear transport of influenza virus ribonucleoproteins”. In: *Journal of virology* 70.12 (1996), pp. 8391–8401.
- [19] J. S. Rossman and R. A. Lamb. “Influenza virus assembly and budding”. In: *Virology* 411.2 (2011), pp. 229–236.
- [20] E. Gasteiger et al. *Protein identification and analysis tools on the ExPASy server*. Springer, (2005).
- [21] S. V. Bourmakina and A. García-Sastre. “The morphology and composition of influenza A virus particles are not affected by low levels of M1 and M2 proteins in infected cells”. In: *Journal of virology* 79.12 (2005), pp. 7926–7932.
- [22] B. Thaa, A. Herrmann, and M. Veit. “The polybasic region is not essential for membrane binding of the matrix protein M1 of influenza virus”. In: *Virology* 383.1 (2009), pp. 150–155.
- [23] P. Gómez-Puertas et al. “Influenza virus matrix protein is the major driving force in virus budding”. In: *Journal of virology* 74.24 (2000), pp. 11538–11547.
- [24] C. Elleman and W. Barclay. “The M1 matrix protein controls the filamentous phenotype of influenza A virus”. In: *Virology* 321.1 (2004), pp. 144–153.
- [25] D. Saletti. “The role of M1 matrix protein in influenza C virus budding”. MA thesis. Chalmers University of Technology, (2015).
- [26] Y. Muraki et al. “Identification of an amino acid residue on influenza C virus M1 protein responsible for formation of the cord-like structures of the virus”. In: *Journal of general virology* 85.7 (2004), pp. 1885–1893.
- [27] V. Brevnov, N. Fedorova, and A. Indenbom. “Effects of pH on the adsorption of the viral matrix protein M1”. In: *Biochemistry (Moscow) Supplement Series A: Membrane and Cell Biology* 9.2 (2015), pp. 84–91.
- [28] J. Fontana et al. “Structural changes in influenza virus at low pH characterized by cryo-electron tomography”. In: *Journal of virology* 86.6 (2012), pp. 2919–2929.

-
- [29] A. Harris et al. “The crystal structure of the influenza matrix protein M1 at neutral pH: M1-M1 protein interfaces can rotate in the oligomeric structures of M1”. In: *International Congress Series*. Vol. 1219. Elsevier. (2001), pp. 405–410.
- [30] R. P. Richter, R. Bérat, and A. R. Brisson. “Formation of solid-supported lipid bilayers: an integrated view”. In: *Langmuir* 22.8 (2006), pp. 3497–3505.
- [31] E. T. Castellana and P. S. Cremer. “Solid supported lipid bilayers: From biophysical studies to sensor design”. In: *Surface Science Reports* 61.10 (2006), pp. 429–444.
- [32] M. C. Dixon. “Quartz crystal microbalance with dissipation monitoring: enabling real-time characterization of biological materials and their interactions”. In: *Journal of biomolecular techniques: JBT* 19.3 (2008), p. 151.
- [33] C. Lu and A. W. Czanderna. *Applications of piezoelectric quartz crystal microbalances*. Elsevier, (2012).
- [34] A. Granéli et al. “Formation of supported lipid bilayer membranes on SiO₂ from proteoliposomes containing transmembrane proteins”. In: *Langmuir* 19.3 (2003), pp. 842–850.
- [35] F Höök et al. “The dissipative QCM-D technique: interfacial phenomena and sensor applications for proteins, biomembranes, living cells and polymers”. In: *Frequency and Time Forum, 1999 and the IEEE International Frequency Control Symposium, 1999., Proceedings of the 1999 Joint Meeting of the European*. Vol. 2. IEEE. (1999), pp. 966–972.
- [36] I. Reviakine, D. Johannsmann, and R. P. Richter. “Hearing what you cannot see and visualizing what you hear: interpreting quartz crystal microbalance data from solvated interfaces”. In: *Analytical chemistry* 83.23 (2011), pp. 8838–8848.
- [37] F Höök et al. “Energy dissipation kinetics for protein and antibody-antigen adsorption under shear oscillation on a quartz crystal microbalance”. In: *Langmuir* 14.4 (1998), pp. 729–734.
- [38] D Ausserré and M.-P. Valignat. “Surface enhanced ellipsometric contrast (SEEC) basic theory and $\lambda/4$ multilayered solutions”. In: *Optics express* 15.13 (2007), pp. 8329–8339.
- [39] A. Gunnarsson et al. “Time-resolved surface-enhanced ellipsometric contrast imaging for label-free analysis of biomolecular recognition reactions on glycolipid domains”. In: *Analytical chemistry* 84.15 (2012), pp. 6538–6545.
- [40] L. V. Chernomordik and M. M. Kozlov. “Protein-lipid interplay in fusion and fission of biological membranes*”. In: *Annual review of biochemistry* 72.1 (2003), pp. 175–207.
- [41] T. O. Edinger, M. O. Pohl, and S. Stertz. “Entry of influenza A virus: host factors and antiviral targets”. In: *Journal of General Virology* 95.2 (2014), pp. 263–277.

- [42] K. K. Lee. “Architecture of a nascent viral fusion pore”. In: *The EMBO journal* 29.7 (2010), pp. 1299–1311.

A

Supporting information

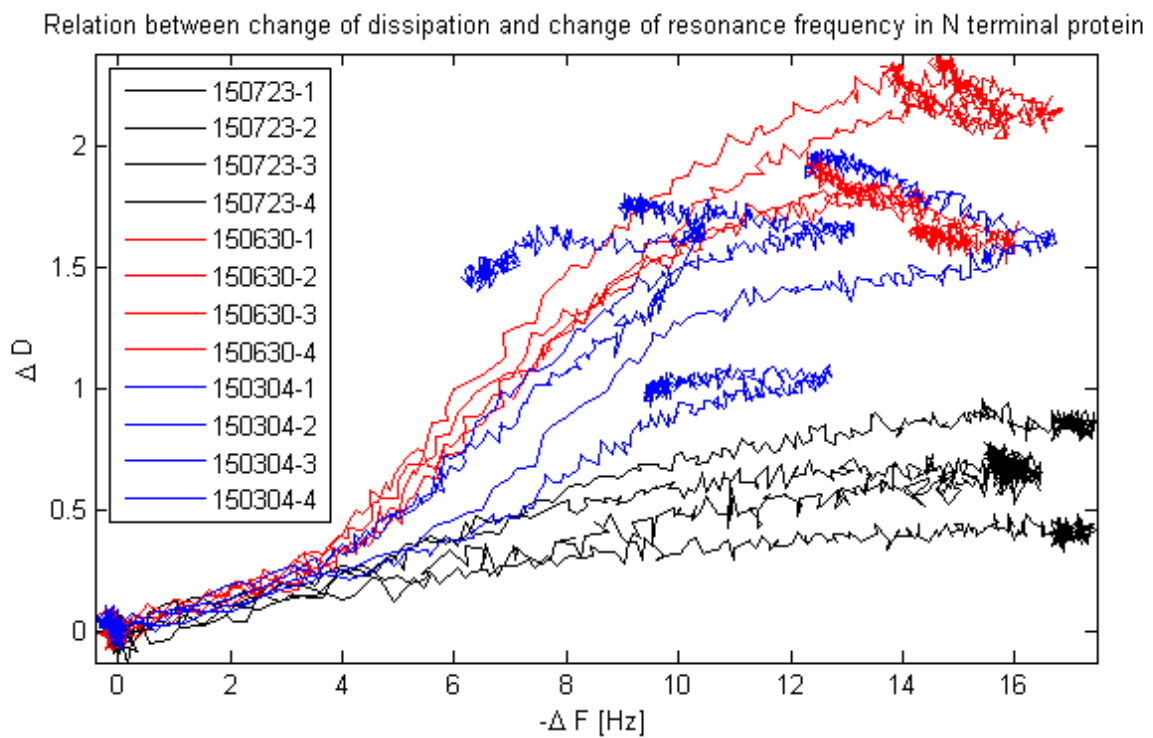


Figure A.1: *QCM-D* data of *N*-terminal $M1_C$ during binding and release.